Chemical Physics Letters 843 (2024) 141190

Contents lists available at ScienceDirect

Chemical Physics Letters

journal homepage: www.elsevier.com/locate/cplett

Frontiers article

The known-unknowns of anomalous underscreening in concentrated electrolytes

Gareth R. Elliott [a], Kasimir P. Gregory [b,c], Hayden Robertson [a], Vincent S.J. Craig [b], Grant B. Webber [d], Erica J. Wanless [a], Alister J. Page [a,*]

[a] School of Environmental and Life Sciences, The University of Newcastle, Callaghan, 2308, NSW, Australia
[b] Department of Materials Physics, Research School of Physics, Australian National University, Canberra, 0200, ACT, Australia
[c] Division of Biomedical Science and Biochemistry, Research School of Biology, Australian National University, Canberra, 0200, ACT, Australia
[d] School of Engineering, The University of Newcastle, Callaghan, 2308, NSW, Australia

HIGHLIGHTS

- Anomalous underscreening is the experimentally-observed phenomenon in which the electrostatic decay length increases with ionic strengths in a manner that cannot be explained via electrolyte theories or simulations.
- We present a comprehensive review of recent theoretical and experimental work aiming to understand anomalous underscreening in concentrated electrolytes.
- We highlight numerous factors that, while potentially important to understanding this phenomenon, have not yet been examined by those working in this field of research.

GRAPHICAL ABSTRACT

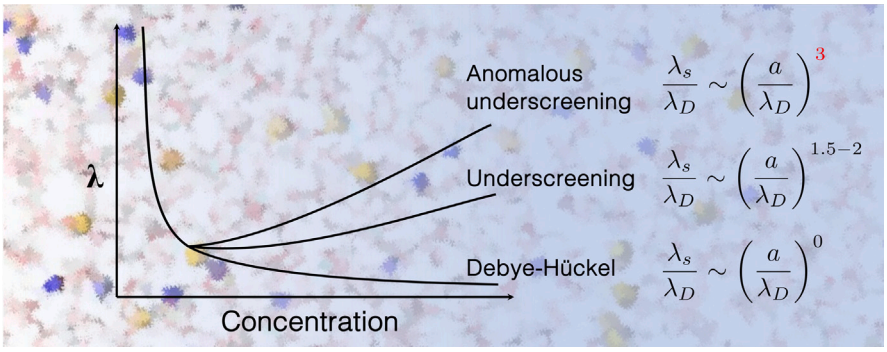

ARTICLE INFO

Keywords:
Electrolytes
Underscreening
Debye–Hückel
Quantum mechanics
High concentration
Ionic liquids
Deep eutectic solvents
Kirkwood point
Hypersaline

ABSTRACT

Electrolytes are central to life and technology but lack complete understanding. Recent experiments with highly concentrated electrolytes have revealed electrostatic decay lengths orders of magnitude larger than those predicted by theory and simulation. This phenomenon, dubbed 'anomalous underscreening' and its origin is still lack a comprehensive understanding. Herein we provide a perspective over recent developments in this field and discuss phenomena that, while potentially pertinent to electrolyte underscreening, are yet to be fully explored - i.e. the 'known-unknowns' of electrostatic underscreening in concentrated electrolytes.

1. Introduction

Electrolytes are of fundamental importance to a vast array of chemical, biological and physical phenomena. They are central to power storage and green energy technologies (e.g. batteries [1–3] and supercapacitors [4–6]), global geophysical phenomena (e.g. weather [7] and oceans [8–10]) and underpin modern agriculture (e.g. *via* fertilisers and

* Corresponding author.
E-mail address: alister.page@newcastle.edu.au (A.J. Page).

https://doi.org/10.1016/j.cplett.2024.141190
Received 3 December 2023; Received in revised form 5 March 2024; Accepted 6 March 2024
Available online 12 March 2024

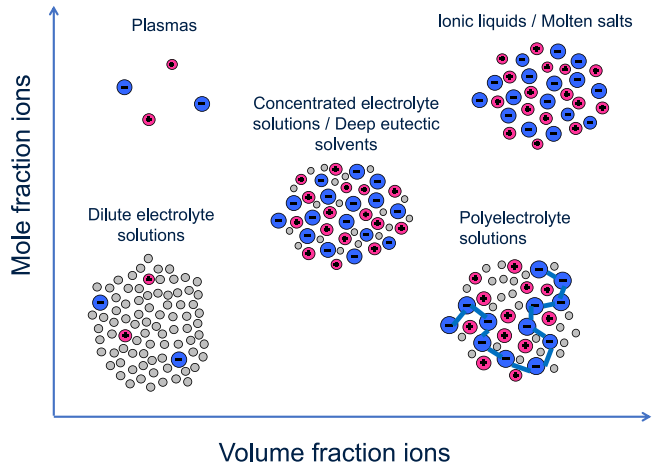

Fig. 1. The spectrum of electrolytes, comprising systems that include or consist entirely of charged species that interact with each other via Coulomb interactions. The density of the charges influences how strong these interactions are, and can be visualised as volume fraction (i.e. density of all species) and mole fraction (number of the species that are ions). Plasmas, while not being an electrolyte, are included for comparison since theoretical treatments of electrolytes share some commonalities [41].

nutrients) [11]. Indeed, life as we know it would not exist without electrolytes [12–15].

Electrolytes comprise charged atomic or molecular species that are dominated by long-range Coulomb interactions. They can exist with other species present (i.e. solvents) and at various concentrations, and this leads to a range of systems that include dilute electrolytes, concentrated ("hypersaline" or "salt-in-solvent") electrolytes [16–19], polymer-based electrolytes [20–26], polyelectrolytes [27–30], deep eutectic solvents (DES) [31,32], ionic liquids (ILs) [33] and molten salts [34] (Fig. 1). Each of the systems shown in Fig. 1 are themselves active areas of research. However, they are unified in the sense that they manifest "ion-specific" physicochemical phenomena [35–39], whereby behaviour and properties are determined by the identity of the ions present, not just their charge or concentration. For such systems the addition of ions do not merely perturb their properties, it drives fundamental changes to them, even at low electrolyte concentration [40].

The presence of ions in solvents generates substantial electric fields [42]. Intermolecular interactions within electrolytes are therefore predominantly Coulombic. While the Coulombic potential from a lone charge in vacuum (or dielectric medium) decays as $1/r$ (where r is the radial distance from the charge), in an electrolyte the potential decays more rapidly due to the presence of other ionic and molecular species and their collective interactions and motions. Indeed, ions in solvents also alter solvent-solvent interactions [43–51], including long-range orientational correlations [52–55]. These local electric fields drive the diffusion of mobile charges to achieve local charge neutrality, a phenomenon known as screening [56]. The most commonly employed model of this phenomenon is the well-known Debye–Hückel [57] (DH) theory (discussed further in Section 2), which predicts in dilute electrolytes a shorter-ranged decay of the form $e^{\alpha r}/r$ [58,59]. The constant α here modulates the length scale of the decay and is a proxy for the extent of the Coulombic screening provided by the surrounding dielectric medium. The length scale associated with this screening is $\lambda_{\mathrm{D}} = 1/\alpha$, which is the distance over which the potential decays to $1/e$ of its initial value [60] - this distance is commonly known as the screening length, or Debye length.

The screening length is a critical property of any electrolyte and is known to influence the conformation and stability of colloidal particles [61–64], lipid phases [65], enzymes [66] and DNA [67,68]. Even fundamental properties of electrolytes, such as conductivity [69–73] and double layer structure [74–76], are influenced by the decay length of the local electrostatic potential. A recent review has also discussed the link between the double layer structure and electrocatalytic activity [77]. Beyond dilute concentrations however, deviations from the prediction of DH theory are observed. This is clearly seen in Fig. 2, which shows measured screening lengths as a function of concentration contradict the predictions of DH theory (dashed line). This deviation is known as underscreening (i.e. the mean electrostatic potential is screened *less* than predicted by DH theory, i.e. it is "under" screened). However, the magnitude of this phenomenon varies between theory and experiment (and between experiments themselves). This has led to underscreening being classified as either *normal* or *anomalous* [78] (see Fig. 2).

To date, no satisfactory explanation that unifies observations of anomalous underscreening with theoretical predictions has been proposed. In this perspective, we therefore summarise recent theoretical and experimental investigations of underscreening in electrolytes. We begin by detailing the key classical theories describing electrostatic interactions in electrolytes (Section 2) and the theoretical origins of underscreening (Section 3). Experiments demonstrating anomalous underscreening are discussed in Section 4. We conclude the perspective by presenting results that highlight the importance of (so-far overlooked) factors related to underscreening, to highlight potential avenues of future research into this intriguing phenomenon (Section 5).

2. Conventional electrolyte models: Poisson–Boltzmann and Debye–Hückel theories

The conventional models of electrolytes are derived from the Poisson equation, which relates the electrostatic potential (ψ) to the charge density (ρ) in a dielectric medium [58,106]:

$$-\varepsilon_0\varepsilon_r\nabla^2\psi(r) = \rho(r) \tag{1}$$

Here the relative permittivity of the medium is ε_{r}, ε_0 is the vacuum permittivity and ∇^2 is the Laplacian operator. A solution to Eq. (1) can be obtained by considering a reference ion and computing Coulombic interactions with other point-charge ions in the system to give the charge density $\rho(r)$. Assuming Boltzmann statistics gives the Poisson–Boltzmann (PB) equation itself:

$$-\varepsilon_0\varepsilon_{\mathrm{r}}\nabla^2\psi(r) = qn^b e^{-q\psi(r)/k_BT} \tag{2}$$

where q is the reference ion charge, n^b is the ensemble number density, k_{B} is the Boltzmann constant, and T is the temperature. General solutions to the PB equation must be calculated numerically. However, in the case where the potential is small, the exponential can be linearised and the solution written in closed form [58]. This linearisation of Eq. (2) is otherwise known as the Debye–Hückel equation [57,58]:

$$\nabla^2\psi_i(r) = \begin{cases} 0, & 0 < r < a \\ \kappa_{\mathrm{D}}^2\psi_i(r), & r \geq a \end{cases} \tag{3}$$

where a is the diameter of the reference ion. The eigenvalue κ_{D}^2 of this equation is given by:

$$\kappa_{\mathrm{D}}^2 = \frac{1}{k_{\mathrm{B}}T\varepsilon_{\mathrm{r}}\varepsilon_0}\sum_j q_j^2 n_j^b \tag{4}$$

with the Debye length (electrostatic decay length) related by $\lambda_D = \kappa_D^{-1}$. For an electrolyte with known concentration, Eq. (4) can be re-written (using $\lambda_{\mathrm{D}} = \kappa_{\mathrm{D}}^{-1}$) as:

$$\lambda_{\mathrm{D}} = \sqrt{\frac{k_BT\varepsilon_r\varepsilon_0}{2q_e^2N_{\mathrm{A}}I}} = \frac{1}{\sqrt{8\pi\lambda_{\mathrm{B}}N_{\mathrm{A}}I}} \tag{5}$$

where $I = \sum_j z_j^2 c_j^b/2$ is the ionic strength, $c_j^b = n_j^b/N_{\mathrm{A}}$ is the bulk concentration of species j (in mol/m^3) with formal charge z_j, and q_e is the electron charge. The equality on the right hand side is an alternate definition of λ_{D} which uses the Bjerrum length, λ_{B}, which is

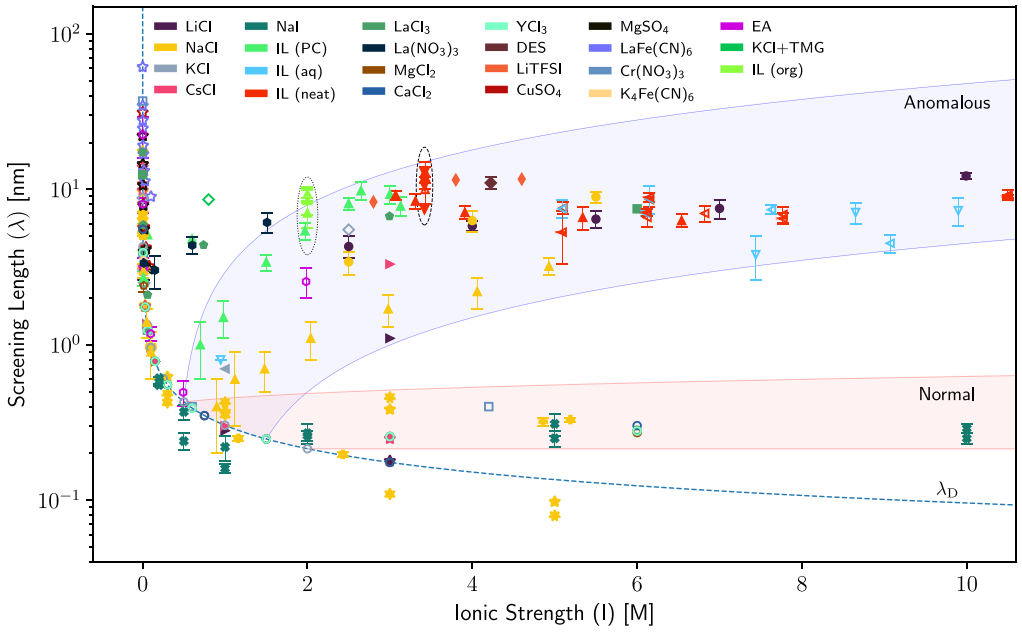

Fig. 2. Concentrated electrolytes exhibit underscreening, whereby the observed screening length λ_S becomes larger than that predicted by Debye–Hückel theory (λ_D). A collation of experimental and theoretical results indicates underscreening and anomalous underscreening in various concentrated electrolytes. Data series are coloured according to salt/solution, while symbols indicate the source of the data and the experimental/theoretical technique used. Data corresponds to aqueous solutions at 298 K unless otherwise specified. Triangles or polygons refer to surface force balance (SFB) experiments for various electrolytes: ▲ Ref. [79], ◀ Ref. [80], ▶ Ref. [81], ▼ Ref. [82], △ Ref. [83], ▽ Ref. [84], ◁ Ref. [85], ◀ Ref. [86], ◁ Ref. [87], △ Refs. [88,89], ▲ Ref. [90], ■ Ref. [91], ⬟ Ref. [92], ⬢ Ref. [93], ◆ Ref. [94], ◇ (with 0.5 M TMG) Ref. [95], ⧫ Ref. [96], □ Ref. [91], ⬠ Ref. [97], ⬡ Ref. [98]. Stars refer to atomic force microscopy (AFM): ★ Ref. [99], ★ (pH fixed equal to 9) Ref. [99], ★ (temperature set to 318 K) Ref. [99], ☆ Ref. [100]. Filled circles (●) refer to fluorescence measurements from Ref. [101], open circles (○) refer to λ^* from Ref. [102]. All-atom molecular dynamics (MD) simulations are given by × Ref. [103] and + Ref. [104]. The dashed ellipse highlights SFB measurements on $[C_4C_1im][NTf_2]$ (▼, △) where the applied potential was varied [82,83], showing the resulting variation in the value of λ_S within the anomalous regime. The dotted ellipse highlights the variation of λ_S determined from 2 M solutions of $[C_4C_1pyrr][NTf_2]$ (▲, △) in several organic solvents [79,89]. Several chemicals are abbreviated as follows: propylene carbonate (PC), trimethylglycine (TMG), ethanolamine (EA). The density of $[C_4C_1im][NTf_2]$ was calculated using data from Ref. [105].

the distance at which the *unscreened* electrostatic interaction energy is equivalent to the thermal energy k_BT:

$$\lambda_B = \frac{q_e^2}{4\pi k_B T \varepsilon_r \varepsilon_0} \tag{6}$$

Both Eqs. (2) and (5) predict that screened electrostatic potential around the reference ion decreases monotonically, as determined by the unique decay length λ_D. This decay length itself is predicted to decrease with increasing ionic strength. To gauge the effect of the linearisation of Eq. (2) (i.e. using the DH instead of the PB theory), activity coefficients γ obtained using both theories are compared in Fig. 3(a) [107]. This figure gauges the influence of linearisation of the PB equation via the ratio γ_{PB}/γ_{LPB}; any deviation from $\gamma_{PB}/\gamma_{LPB} = 1$ indicates that DH-theory incurs spurious errors in γ. Fig. 3(a) shows that, generally, DH-theory performs reasonably for monovalent (1:1) salts for a wide concentration range. However, it is immediate from this figure that for any non-1:1 electrolyte the DH assumption is not justified, although some of the n:1 or 1:n salts do gain better agreement with the PB theory at higher concentrations. What is not obvious from Fig. 3 is that the PB equation itself becomes increasingly unreliable at higher concentrations due to the assumptions that (a) the distribution of ions surrounding the reference charge is not correlated and that (b) the ions themselves lack finite size effects. Further, atomic force microscopy (AFM) measurements of Smith et al. [100], Fig. 3(b), show deviations from DH theory (as indicated by the ratio $\kappa/\kappa_D \neq 1$) for multivalent ions at much lower concentrations. One of the major reasons for these deviations is that the PB and DH theories treat electrostatics as strictly local; i.e. the potential at a given point is determined only by that point, and not by the surrounding neighbourhood [58,108]. In addition, the absence of finite-size ions in the theory is also detrimental to its predictive utility.

Additionally, the PB/DH theories are used in mean-field descriptions of the electrical double layer (EDL), specifically to describe the charge decay in the diffuse layer. Briefly, the typical mean-field model is known as the Gouy–Chapman–Stern model, which has been built up from various theories beginning with the simple capacitor model of Helmholtz [109,110]. It is now thought to contain a proximal region known as the Stern layer [111], which is split (due to Grahame [112]) into the inner Helmholtz plane (IHP), where adsorbed ions have lost part of their solvation shell, and the outer Helmholtz plane (OHP), where the solvation shells are still intact. This is then followed by the diffuse layer, which is the entry point for the PB/DH theory, as introduced by Gouy [113] and Chapman [114]. The thickness of this layer is colloquially described as coinciding with the bulk screening length (λ), although multiple Debye lengths are actually needed for the decay to reach zero. This model is widely used, and assumed to be comprehensive, despite the shortcomings [77,115–117] due to surface coupling (see Section 5.2) and the limitations of the PB/DH theories.

Concentrated (and multivalent) electrolytes therefore necessitate the use of more sophisticated electrolyte theories. This is also true of the dynamic counterpart, the Debye–Hückel–Onsager (DHO) theory [118–120], which is concerned with predicting electrolyte conductivity. For example, the inclusion of finite-sized ions has recently been shown to give reasonable agreement with experiment [70,71]. Similarly, various other models based on PB and DH theory aim to improve their predictions to higher concentrations either by adding additional terms describing different physical effects, such as finite size effects [121,122], or by including empirical parameters which may or may not describe physical properties, such as in specific ion interaction theory (SIT) [123,124] and the Pitzer equations [125,126]. Further discussion on the derivations and limits of DH theory has recently been reported by Kontogeorgis and co-workers [107,127,128].

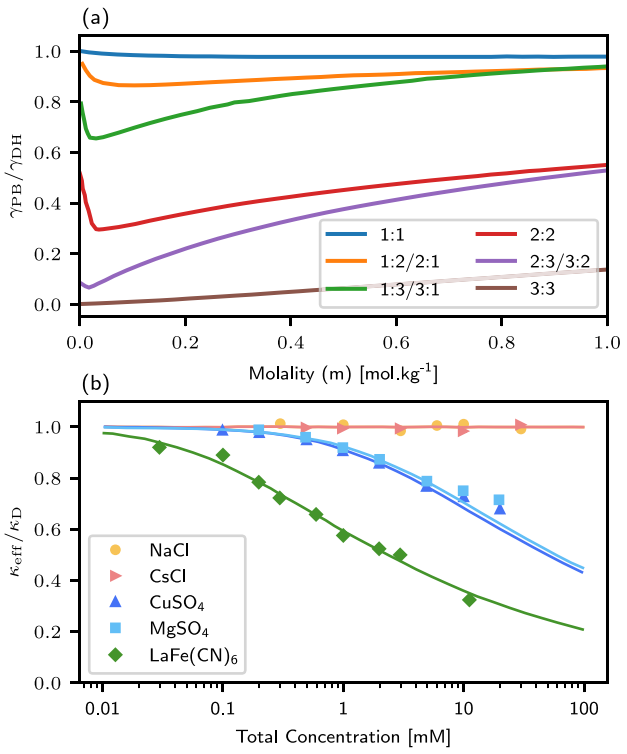

Fig. 3. The shortcomings of conventional electrolyte models. (a) Activity coefficients: γ_{PB} and γ_{DH} give the PB-predicted and DH-predicted coefficients, respectively. Reproduced with permission from Silva et al. [107]. (b) Experimental AFM measurements by Smith et al. [100], showing the significant deviations from DH theory at low concentrations for multivalent electrolytes. Note the different x-scale.
Source: Data reproduced from Refs. [100,107].

3. Beyond Debye–Hückel theory - Origins of underscreening

3.1. The influence of finite ion size

The monotonic electrostatic decay length predicted by the PB and DH equations is the result of considering the reference ion differently to the ions in the surrounding ion cloud (which are treated as uncorrelated point charges). In 1936, Kirkwood presented a theoretical derivation that treated all ions with finite size, and predicted a crossover at high concentrations from the Yukawa-like decay behaviour, to a damped exponential form. This transition point (from monotonic decay to oscillatory decay) bears Kirkwood's name, and arises solely from the finite ion size included in the model. This approach was revisited in a later work by Kirkwood and Poirier [121], and more recently by Kjellander and co-workers, who employed the dressed ion/molecule theory (DIT/DMT) [129–134], which treats all ions consistently as finite sized particles and incorporates nonlocal electrostatics. This statistical mechanical treatment gives the following equation for κ:

$$\kappa^2 = \frac{1}{\lambda} = \frac{1}{k_B T \mathcal{E}_r^*(k)\epsilon_0} \sum_j n_j^b q_j q_j^* \tag{7}$$

where q_j^* is the "dressed" charge of ion species j that accounts for nonlocal electrostatics by taking into account the charges in the neighbourhood of the particle [135]. $\mathcal{E}_r^*(k)$ is given by:

$$\mathcal{E}_r^*(\kappa) = 1 + \frac{1}{\epsilon_0} \int r^2 \left[\frac{\sinh(\kappa r) - \kappa r}{(\kappa r)^3} \right] \chi^*(r)\, d\mathbf{r} \tag{8}$$

and provides a more sophisticated description of the permittivity (compared to the simple relative permittivity ε_r) that is dependent on κ and the polarisation response function $\chi^*(r)$ [136]. Under this framework,

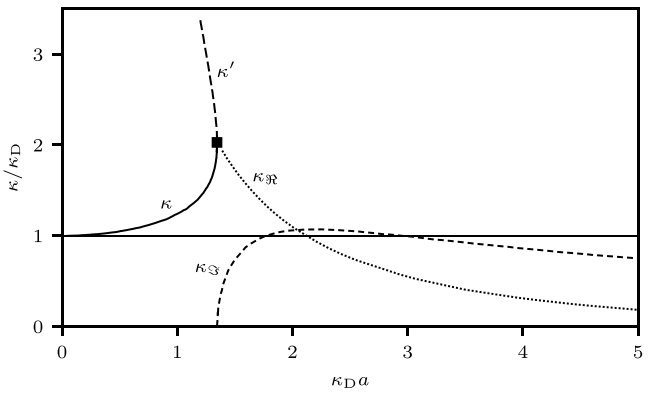

Fig. 4. Solutions to Eq. (9) for a 1:1 electrolyte at room temperature. Deviations from the horizontal line at κ/κ_D indicate deviations from DH theory (i.e. where $\kappa = \kappa_D$). At low concentrations (i.e. low $\kappa_D a$), the dominant solution is κ, however as $\kappa_D a$ increases, κ' will be increasingly non-negligible. At the Kirkwood point (indicated by ■), $\kappa = \kappa'$ and then at higher concentrations the solution becomes complex, with $\kappa = \kappa_\Re \pm i\kappa_\Im$, indicating the onset of the damped oscillatory behaviour. In this theory, the onset of normal underscreening occurs at $\kappa_D a \approx 2$, where $\kappa/\kappa_D < 1$. Redrawn after Kjellander [138].

strongly correlated ions (e.g. ion pairs) will not contribute to q_j^*, but will contribute (as dipoles) to the value of $\mathcal{E}_r^*(k)$ [108].

While these revised theories are analytically exact, if some constraints are imposed (e.g. so that it resembles a DH-like form [137,138], with finite sized particles with dressed/effective charges), the deviation between DH-predicted κ_D and the simplified DIT theory (κ) can be calculated via [138]:

$$\left[\frac{\kappa}{\kappa_D}\right]^2 = \frac{e^a}{1+\kappa a} \tag{9}$$

Eq. (9) gives two solutions, and these are shown in Fig. 4 for a 1:1 electrolyte at room temperature. At low $\kappa_D a$ ($\propto \sqrt{I}$) the electrostatic potential exhibits typical Yukawa decay [139]:

$$\psi_i(r) \sim C_i \frac{e^{-\kappa r}}{r} + C_i' \frac{e^{-\kappa' r}}{r} \tag{10}$$

where C_i and C_i' are constants associated with the two decay lengths $\lambda = 1/\kappa$ and $\lambda' = 1/\kappa'$. Of these, κ dominates as κ' is large and decays quickly. As $\kappa_D a \to 0$, $\kappa \to \kappa_D$ i.e. at very low concentrations DH behaviour is recovered (indicated by $\kappa/\kappa_D = 1$). Interestingly, at non-zero $\kappa_D a$, the decay length of the primary response (κ) is predicted to decay faster than DH theory ($\kappa/\kappa_D > 1$). The theory predicts that κ and κ' will converge at the Kirkwood point (≈1.2 for the example 1:1 electrolyte considered in Fig. 4), at which point the solutions $\kappa = \kappa_\Re \pm i\kappa_\Im$ become complex conjugates (with real and imaginary parts $\kappa_\Re$ and $\kappa_\Im$, respectively). In this regime the electrostatic potential exhibits oscillatory decay (first shown by Kirkwood [140]) such that [139]:

$$\psi_i(r) \sim B_i \cos\left(\kappa_\Im r + \vartheta_i^c\right) \frac{e^{-\kappa_\Re r}}{r} \tag{11}$$

where $1/\kappa_\Re$ is the decay length, $2\pi/\kappa_\Im$ is the wavelength of the oscillation (associated with the particle size(s)) and ϑ_i^c is a phase shift. Importantly, in this regime $\kappa_\Re$ becomes longer than the DH prediction (at $\kappa_D a \approx 2$), a phenomenon known as underscreening — where the screening length is longer than the DH prediction.

The result of Kjellander and co-workers result is not unique, and there have been multiple other notable theoretical approaches [141], and these have been discussed recently by Jäger et al. [142] and Espinosa-Marzal et al. [143]. Similarly, Carvalho and Evans [144,145] and Attard [146] derived theories based on analysis of the Ornstein–Zernike equation [147]; Bazant, Storey and Kornyshev (BSK) [148] used a Landau–Ginzburg treatment; Frusawa [149] and Gavish, Elad and Yochelis [122] used a modified Poisson–Nernst–Planck model, with

the latter work indicating that the onset of oscillatory behaviour is due to both the concentration and the asymmetry in the ion sizes. Ludwig et al. [150] derived an Ising model and Adar et al. [151] used a modified Coulomb kernel incorporating finite sized particles. Rotenberg et al. [152] derived the Landau fluctuation theory for bulk solutions. Additionally, there has been some interest in understanding the effect of a thermal gradient on the screening length [153].

The solution of statistical mechanical theories, such as the Bogoliubov–Born–Green–Kirkwood–Yvon hierarchy [154–157] or the Ornstein–Zernike equation [147], requires appropriate closure [158–160]. For the latter, several well-known closures have been used, such as the hypernetted chain equation, the Percus–Yevick equation and the mean spherical approximation (MSA). Each carries its own assumptions and approximations, and we point the interested reader to Refs. [159,160] for a complete discussion and derivation of the relevant results. Simplistic models of atoms are typically invoked in order to achieve an analytical solution, or even to simplify associated numerical calculations. For example, a common treatment of ions is the primitive model, which considers ions as oppositely charged hard spheres. Adding the additional constraint that all ions have equal size results in the restricted primitive model (RPM), which additionally employs a dielectric solvent medium. Owing to this ansatz the RPM can introduce unphysical artefacts that result in the decoupling of density–density and charge–charge correlations [58,161]. The use of a constant Bjerrum length (which corresponds to unscreened electrostatic interactions, see Section 2) and concentration-independent relative permittivity [43,162,163] is also problematic in this respect.

3.2. Simulating underscreening

Examining electrolyte underscreening via computational simulations is a natural extension to the first-principles treatments discussed in the preceding section, and an increasingly-utilised approach. There are two main approaches that are taken: classical density functional theory (cDFT) and molecular dynamics (MD). What is generally found is that in bulk there is an onset of oscillatory behaviour (Kirkwood point) at a certain concentration, and the prediction of screening in the normal regime (see Fig. 2). The screening length is typically extracted from the predicted densities via a calculation of the total charge correlation function [103,164]:

$$\psi_i(r) \sim g_{zz}(r) = g_{++}(r) + g_{--}(r) + g_{+-}(r) \tag{12}$$

where $g_{++}(r)$, $g_{--}(r)$, $g_{+-}(r)$ are the radial distribution functions of cations–cations, anions–anions and cations–anions respectively. This form can be simplified if a model such as the RPM is used that uses same-size, oppositely charged particles.

3.2.1. Classical density functional theory

cDFT models treat all ions on the same basis and with finite size, and are therefore able to recover the Kirkwood crossover point, and predict the existence of underscreening at high concentrations [142,165–167]. Generally cDFT studies also find agreement with atomistic MD simulations [142,165,168] (see below), but none have shown the presence of anomalous underscreening. However, cDFT does show oscillatory behaviour adjacent to a surface [167–170], consistent with SFB and AFM experiments at small separation distance (see Sections 4.1 and 5.1). Further discussion of cDFT results can be found in the recent paper by Jäger et al. [142]

3.2.2. Molecular dynamics

Many approaches to understanding underscreening (and electrolytes in general) make use of molecular dynamics (MD). These range in sophistication from the RPM in a dielectric continuum, to all-atom MD (with explicit solvent) which includes a more realistic treatment of intra- and intermolecular forces. Coles et al. [103] observed underscreening in bulk NaI(aq), LiCl(aq) and LiTFSI in both aqueous non-aqueous solvents. Their predicted screening lengths are shown in Fig. 5(a) and are in agreement with MSA calculations using the RPM [152]. Similarly, Zeman et al. examined underscreening in aqueous NaCl and $[C_4C_1im][NTf_2]$ in propylene carbonate in both bulk [104] and under confinement with graphene [171]. The very significant size and timescale of these simulations is noteworthy, as is the use of multiple oscillatory functions of the same form as Eq. (11) to determine the electrostatic decay length. An extension of the theory presented in Section 3.1 allows for the existence of multiple decay modes that can be either purely Yukawa (exponential), or oscillatory [58,172]. In the long-range limit, the mode that dominates, and hence measured, is that with the longest decay length. The results of Zeman et al. are depicted in Fig. 5(b), showing the decay lengths obtained from the multiple fitting.

Earlier work by Keblinski et al. [173] probed the phase space of molten and gaseous NaCl and showed the onset of the oscillatory behaviour, with two distinct decay modes clearly coexisting close to this point. This consisted of a short-range oscillatory mode, and a long range monotonic mode, reminiscent of the experiments described in the following section. Notably however, this result was achieved without an interface. The influence of confinement on the screening length in NaCl(aq) was considered by Finney et al. [174], who observed an increase in the screening length at higher concentrations , in line with surface force balance (SFB) results (see below). However, deviations from the DH theory were also observed in the concentration region where there is agreement between theory and experiment. Other investigations using constant chemical potential methods [142] do not find the scaling found by Finney et al., hence these results are deserving of further investigation.

Despite the complexity of the above simulations, the use of coarse grained simulations [104] and even more simplistic models (such as the primitive model with coarse grained solvent [175,176] or dielectric solvent [165,166,177]) capture much of the physics associated with the screening length [142,166]. The agreement seen between simulations of different complexities is most likely due to the Coulomb force dominating the behaviour. Notably however the multiple decay lengths seen by Zeman et al. are not recovered by these more simplistic treatments. Caution should be used to ensure that any MD simulation considers a region of the phase space probed experimentally, as pointed out by Härtel et al. [78].

4. “Anomalous” underscreening

Whilst the theory predicting underscreening (and other non-DH behaviour, such as the Kirkwood point) has been around for a number of decades, several experiments in the last 10 years have revealed underscreening contrary to predictions from theory and simulations discussed above (Fig. 2). Such underscreening is known as “anomalous” underscreening, to be differentiated from the “normal” underscreening that is predicted by theory [78]. It is thought to be of electrostatic origin [178] and was originally highlighted by SFB measurements of aprotic ILs by Gebbie et al. [83,179], who attributed anomalously large screening lengths to ion-clustering within the IL. It was hypothesised that the number of ‘free ions’ in the bulk is much lower than expected, and so the screening length is consequently larger. This hypothesis was made in the context of the then-ongoing debate regarding the ionicity of ILs [180–182]. However, mounting evidence in aqueous and non-aqueous electrolytes indicates that it is a general phenomenon not limited to ILs, and so is unlikely due to strong ion clustering. Moreover, to our knowledge scattering experiments have failed to detect the existence of long-lived clustering in ILs and concentrated electrolytes.

The hallmark of anomalous underscreening is the scaling exponent $\xi = 3$ in the following equation proposed by Lee et al. [89]:

$$\left(\frac{\lambda_S}{\lambda_D}\right) \sim \left(\frac{a}{\lambda_D}\right)^{\xi} \tag{13}$$

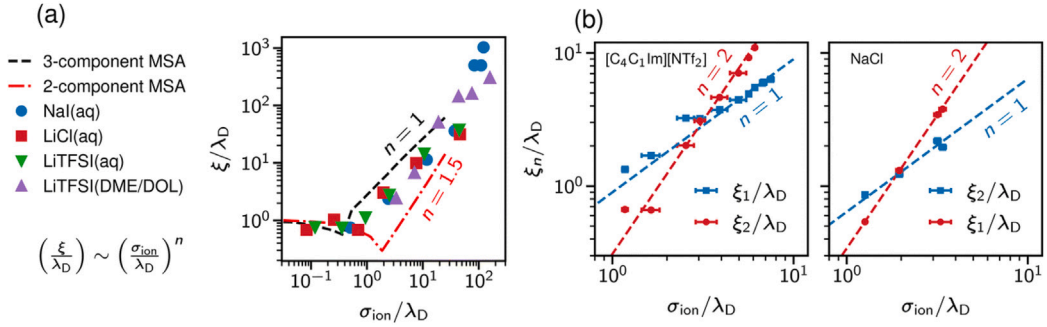

Fig. 5. Bulk MD simulation results using classical force fields, showing the scaling of the screening length (here denoted as ξ, rather than λ). The x-axis is in units of σ_{ion}/λ_D, where σ_{ion} is the ion size. (a) Coles et al. [103] (and the MSA results of Rotenberg et al. [152]). (b) Zeman et al. [104].
Source: Figure used with permission from Ref. [142].

where λ_S is the measured screening length and ξ an empirically-determined constant. Eq. (13) describes underscreening when $a/\lambda_D > 1$ (note $a/\lambda_D \propto \sqrt{I}$). DH behaviour corresponds to $\xi = 0$ in this equation, i.e. $\lambda_S = \lambda_D$, while underscreening corresponds to $\xi > 0$. Generally theory and simulations detailed in the preceding discussion find $1 \leq \xi \leq 2$, whereas anomalous underscreening finds $\xi \approx 3$ [78,89,178]. Despite some promising theoretical treatments aimed at elucidating anomalous underscreening, no simulation or theory has yet been able to explain this phenomenon consistently with experiment. The fact that experimental observations of anomalous underscreening are based on exclusively interfacial techniques (the majority of which are SFB measurements) suggests that anomalous underscreening itself could be an artefact of such techniques. Indeed, one recent article has suggested that the SFB only resonates with particular modes of the correlation function [183]; there is still a strong possibility that the presence of an interface itself may be required for anomalous underscreening to manifest. Nevertheless, simulated interfaces fail to produce anomalous underscreening according to the power law of Eq. (13) [171] (we return to a discussion of surface chemistry and confinement in Section 5). Therefore, to date, no satisfactory explanation for the existence of anomalous underscreening has been established in the literature. The discussion below therefore reviews the current state of experimental and theoretical investigations aimed at understanding anomalous underscreening.

4.1. Surface force balance measurements

The surface force balance is an experimental technique to measure the forces in a liquid by imposing compression or rarefaction between two crossed cylinders. There exist several variants of the technique, and some of these are known as a surface force apparatus (SFA). While there are subtleties in the implementations, herein we refer to all these as SFB, as was done in the recent review by Lin and Klein [185]. We also draw the readers attention to a very recent, and comprehensive, introduction and review of the SFA/SFB technique [186].

Just over a decade ago, SFB experiments were performed by Gebbie et al. on the IL $[C_4C_1im][NTf_2]$ confined between mica and gold [83], where the concentration of ionic species (ignoring any ion pairing/clustering) is 3.43 mol/L at 298.15 K. This gives a predicted Debye length (λ_D) of 0.06 nm. However, in fitting the decay of the force profile, they determined a screening length $\gtrsim$ 10 nm at all the applied potentials tested. A subsequent work probing the effect of temperature repeated these experiments using the ILs $[C_2C_1im][NTf_2]$ and $[C_3C_1im][NTf_2]$. These experiments revealed that the screening decreased with increasing temperature, in contrast to that predicted by Eq. (5) [179]. While the relative permittivity does vary with temperature [43,187–189], the amount of variation of the permittivity for similar ILs [189] is less than the temperature variation, so with increasing temperature $\varepsilon_r * T$ still increases, and so λ_D is still predicted to increase. The authors suggested the possibility that IL ion pairs have a significant energy barrier for dissociation, meaning that only the ions that underwent thermal excitation to the free states would contribute to screening. The concentration of these free ions must be significantly reduced compared to the total number of ionic species, i.e. <0.1% [83]. A review of several of the initial experiments also pointed out that if anomalous underscreening was due to entropic changes, this would be purely repulsive and would increase with temperature [178,190].

Independent SFB measurements by Smith et al. [79] extended the results of Gebbie et al. from ILs to electrolytes in general. Smith et al. examined aqueous NaCl, neat $[C_4C_1pyrr][NTf_2]$, $[C_4C_1pyrr][NTf_2]$ in propylene carbonate and some additional neat ILs, and showed a minimum electrostatic decay length (MEDL) at ≈1 mol/L for both the diluted IL and $NaCl_{(aq)}$. At concentrations lower than this threshold, the decay length decreased in agreement with DH predictions, whereas above it the screening length increased. Lee et al. [88,89] subsequently showed that ion-specificity in this phenomena could be removed by considering normalised ion sizes and a relative permittivity fitted from experiment (see Fig. 6(a)), meaning that the observed anomalous screening lengths were consistently characterised by an exponent in Eq. (13) of $\xi = 3$ when $a/\lambda_D > 1$. Unfortunately, because data for large a/λ_D is difficult to obtain (particularly due to solubility limits), these experiments probed underscreening primarily within a single decade of ionic strength, as noted recently by Härtel et al. [78].

Multiple other SFB experiments have since been reported using mica interfaces with electrolytes ranging from water-in-salt solutions (water in LiTFSI) [96], DES [94], IL systems [82,84,86,191–193] and aqueous solutions [81,95]. Such experiments consistently indicate the presence of anomalous $\xi \approx 3$ underscreening. A selection of these results is shown in Fig. 6(a). We note that at high a/λ_D, a deviation from this trend is seen, and while this could be due to the difficulty in estimating the diameter of the complex-shaped ILs [89], it is possible it also shows a break from the trend, so further investigation of this phenomenon at high a/λ_D values, especially if it can be done with spherical or symmetric ions, would be a useful endeavour.

SFB force curves generally reveal short-range ordering at the solid–liquid surface for small surface separations (indicated by oscillatory forces), followed by a long monotonic decreasing 'tail'. When plotted on a log-linear curve, the gradient of the tail can be used to derive the screening length. Typically, changes in concentration, humidity, temperature or composition only affect the short range behaviour in such force curves [86,192,193]. Lhermerout et al. [191] undertook experiments at different approach rates of the SFB surfaces, and determined that hydrodynamic forces were not the cause of the anomalous screening lengths, despite examples of very slow equilibration dynamics, even up to or greater than 20 h [84,87,192]. Additionally, the presence of water, while showing a marked effect on some properties of ILs [33,194], appears to only have a minor effect on the decay length, and appears generally to cause a decrease of λ in ILs [84,192,195]

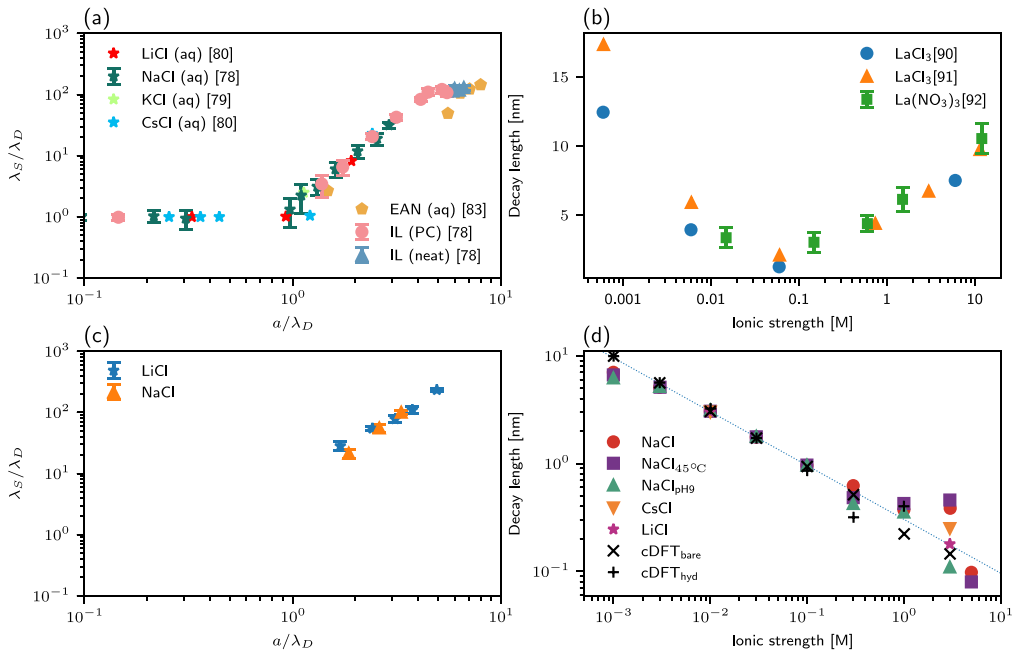

Fig. 6. Experimentally-observed anomalous underscreening. (a) Shows a selection of SFB experimental results for 1:1 electrolytes plotted as λ_S/λ_D vs. a/λ_D, showing the $\xi = 3$ scaling for $a/\lambda_D > 1$. (b) Decay lengths extracted from SFB experiments by Han et al. [93], and by Han et al. from other works [91,92], and plotted against ionic strength, showing the increase in screening length occurring after a minimum electrostatic decay length (MEDL) at ≈0.06 M ionic strength. (c) Fluorescence measurements from Gaddam and Ducker [101] with the same x-axis as in (a). (d) AFM measurements of various aqueous solutions by Kumar et al. [99].
Source: Data extracted using the tool by Rohatgi [184] and reproduced from Refs. [91–93,99,101].

and DES [94]. Similarly, while applied external potentials perturb electrostatic screening, they do not remove the observation of anomalous underscreening, for both mica-IL-gold [83] and mica-IL-mercury interfaces [82,196]. This suggests perhaps that the electric field from the surface need not be particularly strong across the apparatus for the anomalous underscreening to manifest. While the applied potential and surface chemistry (see Section 5.3) can cause variations in the screening, the choice of spring stiffness can also have a marked impact on the ability to resolve the long range forces [185,197].

Despite the predominant use of interfacial force measurements in this field, there have been suggestions that anomalous underscreening is a bulk phenomenon. Considering the SFB measurements of Smith et al. [79], which employed a neat IL (concentration ≈3.3 M), a screening length of 8.4 nm was reported. Taking one screening length from both confining surfaces gives a separation of 16.8 nm, covering almost the entire force-distance profile reported in that study. In this case the measurement therefore cannot be considered a *bulk* measurement. In contrast, the 2 M NaCl solution exhibited a screening length of only 1.1 nm, which corresponds to an overlap separation of 2.2 nm. Hence the majority of force-distance profile is outside at least one decay length. While the potential of the diffuse layer will not have completely decayed across only one decay length (see Section 2), the measurement will be less perturbed by the surfaces at greater separations, allowing for the possibility that true bulk behaviour is being measured. The respective contributions of the bulk and solid/liquid interfaces to anomalous underscreening therefore remain to be elucidated completely. Additional evidence was also provided by Lee et al. [89], showing agreement between calculations of the excess chemical potential (μ_{ex}) compared to that of bulk measurements (derived from the activity coefficients via $\mu_{ex} = k_B T \ln(\gamma)$), although Zeman et al. [171] have also pointed out that the underlying assumptions of the model used by Lee et al. [89] appears to break down for $a/\lambda_D \gtrapprox 2.5$.

Finally, while most of the recent SFB results have been for 1:1 electrolytes, a recent publication by Han et al. [93] has shown a MEDL at ≈0.06 M ionic strength for the trivalent $La(NO_3)_3$(aq) (i.e. a 1:3 electrolyte) confined between mica surfaces. This study also re-evaluated prior results of $LaCl_3$(aq), also confined by mica, reported by Pashley et al. [91] and Tan et al. [92] (see Fig. 6(b)). These experiments show a clear deviation from DH-predicted screening at lower ionic strength in Fig. 2, and appear to follow the $\xi = 3$ anomalous scaling. Several other SFB experiments also report screening lengths similar in magnitude to these La^{3+} electrolytes. For instance, Adibnia et al. [90] considered $[C_6C_1im][NTf_2]$ in propylene carbonate confined between mica surfaces, while Hallett et al. [95] considered trimethylglycine (TMG) and KCl solutions, also confined by mica surfaces. Screening lengths in the latter study were attributed to a substantial increase in the relative permittivity of the liquid.

4.2. Fluorescence emission spectroscopy

A complementary technique that images an aqueous solution containing fluorescein molecules confined between borosilicate glass and an oxidised silicon wafer [198] has been used by Gaddam and Ducker [101] to study LiCl(aq) and NaCl(aq). The presence of the fluorescein molecule is directly detected by fluorescence emission, enabling the surface excess as a function of surface separation to be determined. By assuming the effect on the double layer of the fluorescein (a large divalent ion present at micromolar concentrations) is only a small perturbation, these experiments yielded screening lengths consistent with those observed by SFB, see Fig. 6(c). Anomalous underscreening is therefore not merely a manifestation of the SFB technique, or the presence of a mica substrate, for that matter.

4.3. Simulations and theoretical approaches

As discussed above, cDFT and atomistic MD approaches generally yield normal $\xi \approx 1 - 2$ underscreening behaviour. Whether or not anomalous underscreening, consistent with experimental observations, can be derived from current theories remains unclear. For instance, the mesoscopic theory of Ciach and Patsahan [199,200] finds some

agreement with the $\xi = 3$ scaling found by experiment, however it has been pointed out [142,151,171] that this is only achieved for $a/\lambda_d > 2.5$, whereas experiments exhibit anomalous underscreening for $a/\lambda_d \gtrapprox 1$ (for a 1:1 electrolyte). This theory also predicts that for $a/\lambda_d > 4$ the value of ξ should increase further, however there does not appear to be any evidence of this trend from experiments. For instance, screening lengths in SFB experiments appear to plateau at high concentrations (see Fig. 6(a)), although we note that the determination of the value of a for IL ions (which dominate this data) is questionable, as this value implicitly assumes that ions are spherical. Similarly, a recent paper by Härtel et al. [78] using molecular dynamics (MD) simulations of ions under the restricted primitive model (RPM) has also suggested good agreement with experiment, but requires the assumption of significant ion pairing (see Section 5.5). However, these MD simulations are in agreement with the Ciach and Patsahan theory, in that at higher a/λ_D, ξ increases. This was also observed by Zeman et al. [171] using the inverted model of Lee et al. [89] and experimental activity coefficient data.

5. The "known-unknowns" of anomalous underscreening

Based on the growing body of evidence discussed above, there are a number of "known-knowns" associated with anomalous underscreening. For instance, anomalous underscreening appears to be a general phenomenon for monovalent electrolytes in aqueous and non-aqueous solvents. It is also observed in molten salts, such as ILs. Nevertheless, there are still many "known-unknowns" regarding anomalous underscreening — factors that are potentially relevant to understanding the origins of anomalous underscreening that are yet to be considered, or resolved completely. The aim of the discussion presented below is to draw attention to these factors, in an effort to highlight possible avenues for future research.

5.1. Interfacial geometry

Interfaces fundamentally influence physicochemical phenomena. Notably, the chemistry and electronic structure of solid surface(s) influences both structural and temporal properties of electrolyte interfaces [178]. For example, it has been shown that reversals in the Hofmeister series for the observation of yield stresses are dependent on the chemical structure of the surface (mica versus alumina) [201,202], with theory suggesting this arises from hydration and nonelectrostatic (i.e. dispersion) effects [203]. Similarly, Schwierz et al. have shown that the ordering of the Hofmeister series depends on the surface charge and the polarity (hydrophobic versus hydrophilic) [204].

As noted above, there is ongoing debate regarding whether or not underscreening is a bulk or interfacial phenomenon. The vast majority of experimental evidence of anomalous underscreening is, however, obtained from interfacial measurements. In this respect, the geometry of the interface itself is also likely a key factor, and the study of electrolytes under confinement has been discussed very recently by several groups [205–207]. Simulations by Zeman et al. [171], which considered electrolyte solutions confined between graphene monolayers, did not yield anomalous underscreening. In contrast, a recent approach by Gurina et al. [208] did indicate some agreement.

The issue of interfacial geometry is succinctly illustrated by comparing SFB results with those obtained using AFM. The former almost exclusively yields anomalous underscreening ($\xi \approx 3$, Eq. (13)), while the latter generally yields normal underscreening ($\xi \approx 1.5-2$, Eq. (13)), as shown in Fig. 2. AFM has been widely used to study ionic solutions and the structure of the solid–liquid interface; it can also be used to measure force-distance information, analogous to the SFB. However, while the SFB typically uses surfaces interacting across the liquid of interest with a radius of ~1 cm, AFM generally utilises a flat surface (upon which the solution of interest is placed) and either a colloid probe (with radius of 1–15 μm) or a bare tip (with radius of curvature, R, of 1–100 nm) interacting across the liquid of interest. Hence there is a higher degree of geometric confinement in the SFB than in the AFM. Smith et al. [100] employed a colloid probe to examine screening in a series of symmetric (i.e. n:n) electrolytes (NaCl, CsCl, $CuSO_4$, $MgSO_4$, $LaFe(CN)_6$) on a silica particle substrate. Results obtained deviated from DH theory for the di- and trivalent salts at low concentrations, while the monovalent salts were in agreement with DH theory over the concentration range studied (0.01–100 mM); a result attributed to the presence of ion pairs. A similar conclusion was reached by Stojimirović et al. [209] for LiCl and tetrabutylammonium chloride (TBAB) in isopropanol. Since the concentration range of these two studies was still <1 M, whether underscreening here is normal or anomalous is unclear. Kumar et al. [99] investigated several aqueous alkali halide solutions (using an AFM tip with $R = 252$ nm) and also failed to observe $\xi = 3$ anomalous underscreening. Instead their measurements were in agreement with cDFT results [165], see Fig. 6(d), and were not sensitive to the identity of the substrate (silica vs. mica). We note here also that only a moderate deviation is seen from the DH prediction itself in these experiments. Silica colloid probe measurements by Hjalmarsson et al. [210] of the IL ethylammonium nitrate (EAN) on a mica surface suggested that anomalous underscreening could be switched on at temperatures above 373 K. This result is contrary to the smooth temperature dependence observed by Gebbie et al. [179] using SFB, and also recent SFB measurements of EAN confined by mica by Fung and Perkin [84] which demonstrated that the long range decay manifests at all temperatures. Potentially, the manner in which temperature is controlled is therefore an important factor [211].

5.2. Surface-adsorbed ions

While the geometry of the interface is a likely factor associated with the manifestation of anomalous underscreening, the dynamics of the electric double layer (EDL) appear less influential. For aqueous solutions with simple inorganic ions, simulations using Brownian dynamics have suggested that the relaxation of the double layer following electron transfer ranged from 0.40 ns at 0.11 M to 0.05 ns at 1.02 M. Additionally, this value decreased when the surface charge density was higher [212]. In contrast, ILs, due to the inherent asymmetry of their constituent ions and higher viscosities, undergo structural relaxations on far longer timescales. For example, Han et al. [87] performed X-ray scattering and SFB measurements on both dry and wet imidazolium-based ILs, and saw layers near the surface form over a timescale of ~24 h. Belotti et al. [213] showed that an electric field persists near the interface (after an initial voltage pulse) for up to 100 h (depending on the IL). The screening length determined by Han et al. was characteristic of anomalous underscreening. Nevertheless, mean field EDL theories are unable to describe correlation effects at high electrostatic strengths, which can be determined by the following parameter due to Netz and coworkers [116,214]:

$$\Xi = \frac{2\pi\sigma\lambda_B^2 q^3}{e} \tag{14}$$

where σ is the surface charge density, q is the ion valence and e the electron charge. For $\Xi \gtrapprox 10$, the correlation effects between the liquid and the surface will be substantial enough to deviate appreciably from the mean field models described earlier [116] (Section 2).

While the Stern layer is generally thought to be a single layer of counter ions, there have been various theoretical treatments that have suggested alternating charge layers adjacent to the surface, causing an oscillatory charge profile (known as overscreening) normal to the interface [74,148]. This is thought to influence the screening length, and recent X-ray reflectivity measurements [215,216] of high concentration aqueous RbCl and RbI on mica suggested that the thickness could extend to ≈2 nm. The exact effect of this surface layering on the nature underscreening has been examined in SFB experiments by Gebbie et al. [83]. In a similar vein, Fung [82] varied the applied

potential across the interface — which would invariably change the structure of the Stern layer (or adjacent overscreening layers) — yet anomalous underscreening was still observed (although the magnitude of the screening length changed). Recent measurements by Belotti et al. [213] using electrochemical methods suggested the presence of overscreening and crowding behaviour, and quartz crystal microbalance (QCM) experiments using aqueous solutions of $[C_4C_1im]Cl$ and NaCl suggested that above ≈1 mol/L, the structure at the surface becomes independent of the concentration [217].

Decoupling the pure geometric effects from the chemical/electrical nature of the interface is extremely challenging experimentally, and this represents a unique opportunity for theoretical and simulation approaches to provide further insight on this point.

5.3. Surface chemistry

The experiments discussed in (Section 4.1) have employed a range of surface materials, e.g. gold, mica, silica and mercury. Of these, mica and silica are the most commonly employed in SFB (and AFM) experiments. However we note that other materials in SFB apparatus, i.e. gold and mercury, also produce anomalous underscreening, and this is irrespective of whether the SFB experiments use symmetric or asymmetric substrate configurations. Nevertheless, disagreement between experiments has led to suggestions that the probe surface influences underscreening itself. In particular, the AFM experiments of Kumar et al. [99] did not show anomalous underscreening using aqueous solutions confined between a silica tip and silica substrate. Switching the silica substrate for mica led to the same conclusion. Similarly, AFM measurements of EAN confined by a silica colloid probe and mica [210] and SFB [84] using mica, yielded contrasting results across a wider range of temperatures. However, the degree to which these differences arise from the silica/mica surface chemistry is yet to be resolved. It is conceivable that they are pertinent; for instance, while mica is cleaved to yield an atomically smooth surface, silica has non-zero surface roughness. While the arrangement of Si^{4+} and the Al^{3+} at the mica surface and subsurface gives rise to structural heterogeneity, inferred from the short-range ordering recently found with an AFM [218], the silica surface is more chemically uniform. Both materials have surface OH groups [218–220] and it has been shown for silica that there is constant protonation and de-protonation of these OH groups. This causes temporal heterogeneity that has been observed on the micrometre scale [116,221]. It is possible that this also occurs on mica, however this is yet to be confirmed. Both materials have low isoelectric points [222] (silica <3, mica <3.5) with experiments typically done above these values, where the surface contains a net negative charge.

5.4. Interfacial confinement

The effects of confinement, especially with respect to the transport of ions, is well established, and has been the subject of several reviews [205–207]. The restriction imposed by the interfacial geometry has also been shown to affect various properties of liquids, as discussed recently [205,206,223]. In particular, the relative permittivity (i.e. the dielectric constant) becomes tensor-valued ($\varepsilon_\perp \neq \varepsilon_\parallel$), and exhibits different real and complex electrodynamic responses [224]. Both $\varepsilon_\perp$ and $\varepsilon_\parallel$ change, and in particular the value of $\varepsilon_\perp$ is reduced overall and exhibits a spatially varying profile away from the surface [206]. Since the forces are measured normal to the surface in both SFB and AFM, we focus on the perpendicular component $\varepsilon_\perp$ in our discussion here.

Confinement causes $\varepsilon_\perp$ to decrease when the separation between the surfaces is <100 nm, as shown in Fig. 7 for both pure water [225–229] and aqueous solutions [230–232]. This result was attributed to a restriction of dipole motion [225], however it has also been suggested that this is caused by the electronic structure of the solid [227]. While the experiments by Fumagalli et al. employed hexagonal boron nitride (h-BN) and graphite surfaces (both hydrophobic), simulations have indicated that it occurs on other substrates [233], including hydrophilic surfaces [234]. It was also shown to occur with other solvents by Motevaselian et al. [235] (Fig. 7). Several theories have been successful in modelling this phenomenon [236,237]. Critically however, the range at which $\varepsilon_\perp$ begins to reduce in Fig. 7 coincides with the distances relevant to the measurement of electrostatic screening lengths using SFB, AFM and fluorescence techniques described in Section 4.1, and this extra contribution is not taken into account in calculations of λ_D in these studies (although the concentration dependence of ε is accounted for).

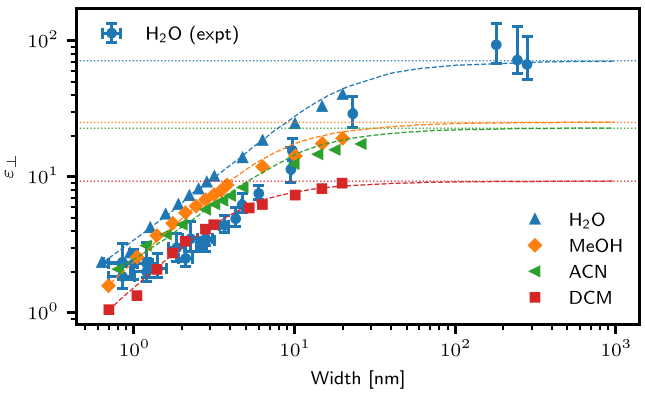

Fig. 7. The perpendicular dielectric permittivity estimated from simulations of several solvents in a graphene slit by Motevaselian et al. [235] and experimental measurements by Fumagalli et al. [225] of water in h-BN/graphite, showing the decrease of the perpendicular relative permittivity due to confinement, which occurs from a significant distance from the surface.
Source: Data reproduced from Refs. [225,235].

The influence of confinement has also been considered from a theoretical standpoint. Recent simulations by Zeman et al. [171] using graphene to confine the electrolyte did not show any stronger scaling than $\xi = 2$, consistent with their earlier work [104]. In an attempt to obtain a better description of the structure around the surface, these authors subsequently used a variety of methods including grand canonical MD [142] and cDFT [142,166], however both methods predicted similar screening lengths from the Kirkwood point ($a/\lambda_D \approx 1$) to around $a/\lambda_D \approx 3$, at which the point the effects of hard-core repulsion become the leading term and became sensitive to solvent choice and ion size. Building on their previous work, Ciach and Patsahan [238] applied their theory to a model slit geometry. They were able to show oscillatory density profiles normal to the interface, and similar to their theory in the bulk, they find some agreement with the $\xi = 3$ scaling, however this is at larger values of a/λ_d than employed experimentally. Ciach and Patsahan's theory is also unable to reconcile the absence of anomalous underscreening seen by Kumar et al. [99] using AFM. It has been suggested by Huang [239], using BSK theory [148], that confinement causes ion-pair dissociation to become unfavourable. Thus, the number of free ions would be vastly reduced and the screening length would therefore increase. Other reports suggest that confinement can cause the violation of charge-neutrality (i.e. where there is unmatched charge within some region) [240,241], and this would be more likely to occur in a SFB due to the confining geometry.

5.5. Ion pairing vs. Ion correlations

There have been many suggestions from various works that the origin of anomalous underscreening is due to ion pairing or clustering [78,83,167,177,239,242], which would decrease the effective concentration of ions (i.e. behave more like a dilute electrolyte). Ion pairing itself is still widely debated, and has been the subject of

numerous reviews [243–249]. The DIT theory discussed in Section 3 allows for a broader description of ion–ion correlations than is incorporated into either the dressed charge q_j^* or $\mathcal{E}_r^*(k)$ (Eqs. (7), (8)). We have also recently shown that for alkali metal chlorides, the ion pair interactions are incredibly dynamic and concentration dependent, and in many cases do not outlive the natural relaxation times of water [250]. This draws into question the importance of ion pairing on macroscopic phenomena such as underscreening. Additionally, there are several works that also suggest that ion pairing cannot be used to explain underscreening. For example, Feng et al. [69] performed non-polarizable MD, and examined how ion pairing and clustering influence dynamic properties of $[C_4C_1im][TFSI]$, and specifically how these were affected by pairing and clustering. These simulations suggested that, while there is a significant association between the cations and anions (corresponding to a free ion percentage of ∼15%), it is not sufficient to explain experimental results. It was similarly found that the degree of ion pairing is insufficient through an analysis of Bjerrum pairing by Adar et al. [251], and by Goodwin and Kornyshev [74] via analysis of the differential capacitance. Further, spectroscopic measurements in aqueous systems do not show an abrupt change about the Kirkwood point, and also do not evidence the amount of ion pairing required to reduce the free ion concentration to result in anomalous underscreening [252–254].

The use of ion–ion correlation, as opposed to ion-pairing, is a more encompassing paradigm, and allows for a rigorous inclusion of nonlocal electrostatics. It also allows for the contribution of any associated species which are still expected to contribute to screening as a dipole (rather than a neutral species). In fact, Kjellander has pointed out that the decay of a solution-phase dipole actually has the same decay behaviour as a lone ion (i.e. a Yukawa-like decay with the same decay length) [255]. The inclusion of zwitterions to a solution is a good test for this, and was shown to markedly increase the screening length [95]. Additionally, Zaurbin and Bier have suggested, based on simulations of a dipolar fluid, that the length scale of investigation can manifest different behaviour for the same system. It has also been pointed out recently [143] that measurements of conductivity, while deviating from Nernst–Einstein conductivity behaviour (due to correlations between the ions), cannot account for anomalous underscreening. Further, ILs do not show sufficient deviations from the behaviour of aqueous KCl solution (assumed fully dissociated) [180]; the authors here have stated that the influence of all the neighbours is more influential than a single pair, and that they appear to move predominantly in an uncorrelated manner. Finally, it has been suggested by several studies that the lifetime of ions is particularly important in describing macroscopic properties. For example, the lifetimes correlate better with the conductivity [256,257] (also found by spectroscopy measurements [73]) and the ionicity [25,26].

5.6. Quantum and many-body effects

Quantum chemical simulations of liquids are difficult, owing to the configurational complexity. However, we suggest (in a similar vein to Parsons et al. [258]) that the absence of quantum mechanical modelling of the liquid state will continue to be a detriment to our understanding of anomalous underscreening. While classical models, which generally use spherical particles, are able to replicate much of the structural information in an electrolyte (e.g. hyperuniformity [200,259,260]), it is plausible that the delocalisation of the electronic density around ions in electrolytes is related to the emergence of underscreening at high salt concentrations. For instance, KS-DFT calculations recently reported by Kathmann and co-workers [42,261] show significant electric fields in aqueous NaCl solutions, and were suspected to underpin crystalloluminescence — the emission of UV light upon crystallisation.

Suggestions of long-range correlations on the nanometre scale [262] and plasma-like collective behaviour [263–265] have also been hypothesised, with frequencies in the THz regime. It is possible geometrical confinement may be required for this to manifest (akin to quantum dots). Apostol was able to derive the $\xi = 3$ scaling law by assuming the existence of dispersive plasmons [263] and suggested that the oscillators are quantum mechanical in nature. It is therefore conceivable that electrolytes at very high concentrations are able to become pseudo-crystalline, leading to infinitely large screening lengths due to long-range ordering [173].

Nuclear quantum effects (NQE) have also not been investigated in the context of anomalous underscreening, despite the marked changes in the properties of condensed phases associated with replacing H_2O with D_2O. In water and other hydrogen-bonding solvents, the smaller mass of ^1H makes it more susceptible to tunnelling meaning that it behaves in a more delocalised manner [266,267]. These effects are particularly significant at low temperature [268]. At room temperature the structural and mean-field properties (e.g. static permittivity) are usually similar [267,269,270], but dynamic and/or instantaneous properties show significant differences, as they are a result of random fluctuations [267].

NQE have been shown to be important in ion solvation [271,272], and the use of D_2O can lead to a significant difference in the solubility limits of various salts [273], as well as differences in the osmotic and activity coefficients [274]. While in bulk solution the effects of heavy water substitution are more pronounced for dynamical properties, recent nonlinear spectroscopic experiments by Dupertuis et al. [275] of 3D confined water determined that the confinement effect of H_2O exists over distances >100 nm. In contrast D_2O was much less affected by the restriction of geometry. SFB experiments by Shrestha et al. [269] have also shown differences in the adhesion energy in these two solvents. Very recently, theoretical work has suggested that a quantum treatment of confined water will induce subtle differences in the behaviour near the surface compared to a classical treatment, and these can propagate to result in non-negligible differences in the electrostatics in the bulk [276]. In light of these results we contend that exploring the effect of NQE on electrostatic screening length should be a priority for future research.

By contrast, a number of studies have elucidated the role of dispersion forces in electrolytes and molten salts. For instance, it is known that better descriptions of SFB experiments are achieved by the inclusion of dispersion interactions [278], and this was used by Pashley et al. to explain the “hydration” force [279]. In ILs, dispersion typically contributes 8%–15% [280–282] of the total IL interaction energy, and so its inclusion is clearly important [283]. However, given the magnitude of the dispersion interaction is less, and it decays faster than the Coulombic interaction (i.e. $1/r^6$ versus $1/r$, respectively), the long-range interactions are expected to be dominated by electrostatics. Given that anomalous underscreening did not manifest in either the all-atom MD by Coles et al. [103] or those of Zeman et al. [104,171], it is unlikely it is the cause of the $\xi = 3$ scaling (since dispersion is included approximately via the molecular dynamics force fields used). Nevertheless, Kjellander and Ramirez [133] have suggested that coupling exists between the electrostatic and dispersion interactions, and this affects the form of the long-range decay. The use of correlated wave function methods that recover the dispersion interactions (e.g. Møller–Plesset Perturbation Theory [284] etc.), or more sophisticated treatments of electron correlation (e.g. the random phase approximation (RPA) [285]) would enable this coupling to be examined directly. A recent FMO-MP2 [286] study of the IL $[C_2C_1im][BF_4]$ demonstrated that the use of such approaches for large-scale simulations of complex condensed phases are now within reach [287]. Similarly, DFT and machine-learning forcefields [288] may assist in this respect, although we note that appropriate care must be taken to select an appropriate level of theory, as many DFT functionals do not properly reproduce the properties of water [289].

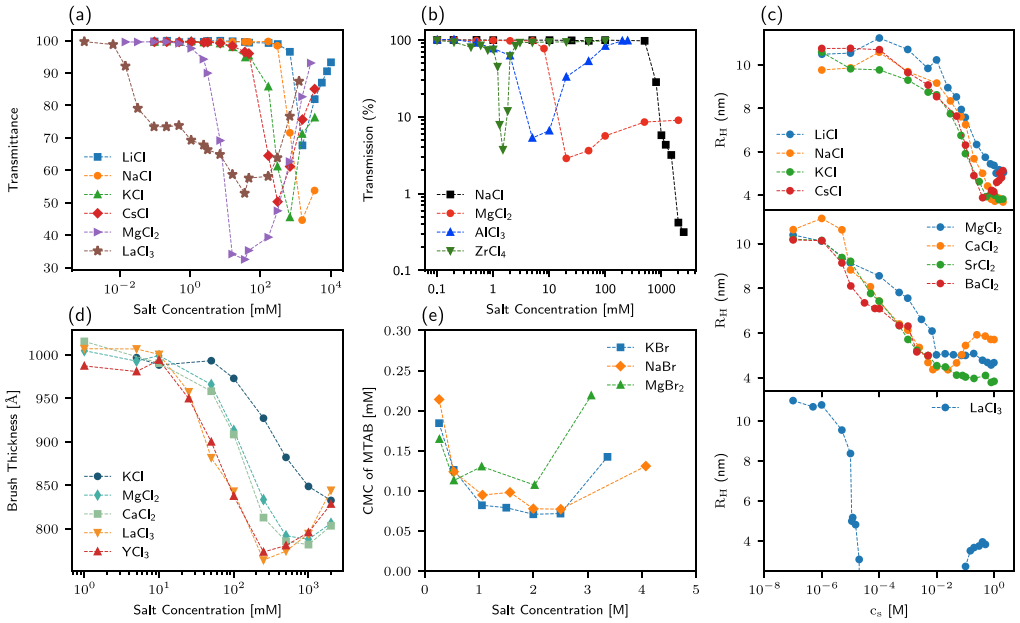

Fig. 8. Examples of reentrant behaviour observed in various soft matter systems. Transmittance of light through a solution containing silica nanoparticles, with various salt solutions by (a) Yuan et al. [61] and (b) Kumar et al. [62]. (c) Contractions and re-swelling of free polystyrene sulfonate with various monovalent (top) divalent (middle) and trivalent (bottom) salts. These data from Jia et al. [277] is plotted without error bars. (d) Reswelling of a polyelectrolyte PMETAC brush by Robertson et al. [102] (e) The effect of salt on the CMC of MTAB, from Yuan et al. [61].
Source: Data reproduced from Refs. [61,62,102,277].

5.7. Multivalent electrolytes

Despite the biological relevance of multivalent ions, there has been relatively few investigations of them in the context of underscreening phenomena. Multivalent electrolytes are generally more challenging than studies of monovalent electrolytes; ideally, measurements are made under conditions of high surface potential, however multivalent electrolytes greatly impact the surface potential under a wide variety of conditions, often adsorbing and leading to charge reversal, complicating investigations of the extent of the double layer. Multivalent electrolytes are also poorly described by the PB theory (see Fig. 3), and are characterised by much stronger ion–ion correlational effects. This has been suggested to result in charge inversion and so-called like-charge attraction between surfaces [290–292]. Nevertheless, the role of ion-clustering and strong Coulomb coupling in this context is yet to be established. A limited number of studies, nevertheless, have demonstrated the existence of underscreening in multivalent electrolytes. For instance the SFB measurements on 1:3 electrolytes discussed in Section 4.1 [91–93] showed a MEDL at a significantly reduced concentration (≈0.06 M) followed by anomalous underscreening. Smith et al. [100] showed deviations from DH theory, but restricted the scope of the study to low ionic strengths. Pashley and Israelachvili [279] performed experiments on alkaline earth metal chlorides and showed for 3 M $MgCl_2$ and 5 M $CaCl_2$ decay lengths of 1.8 nm and 2.0 nm respectively. Parsons et al. [278] suggested these results were due to dispersion, finding good agreement with theory. The absence of an anomalous screening length in these studies is most likely due to a reversal of the surface potential. More recent measurements by Perez-Martinez and Perkin using the dicationic IL $[C_{10}(C_1im)_2][NTf_2]$ also did not show anomalous underscreening [293]. While Kohonen et al. [97] examined NaCl, $MgSO_4$, $K_4Fe(CN)_6$ and $Th(NO_3)_4$ solutions using SFB, concentrations were not sufficiently high to observe underscreening. There is therefore a clear need for surface force measurements of these systems at higher concentrations, particularly since there is a clear impact on so-called reentrant behaviour on polyelectrolyte swelling and other phenomena. We discuss such phenomena in greater detail below.

5.8. Electrochemical approaches

The differential capacitance (DC) of electrolytes has been discussed in the context of underscreening in several studies. The DC of an electrolyte relates the surface charge density to the potential. It has been predicted [148], simulated [169,294] and measured [295], to change due to overscreening and crowding effects at the electrode interface [158,296]. While much of this change is close to the surface, it is likely that these effects can propagate out into the bulk. These predictions and measurements of the DC challenge the massive ion pairing often invoked to explain anomalous underscreening [74]. For instance, Lee et al. [88] used a theoretically derived value of the DC for the IL $[C_2C_1im][NTf_2]$, which was compared to experimental measurements. They found agreement at low concentrations, however there was disagreement as the predicted capacitance (based on their large value of λ) was significantly lower than measured. It is conceivable that the screening length could also be extracted from alternative electrochemical measurements, such as impedance spectroscopy [297], as the Debye length enters such quantities as the Debye time (τ_D) [298]. Despite this opportunity, many, if not all, impedance spectroscopy experiments are performed at concentrations ≤1 M, likely due to the reasons outlined by Borodin et al. [17]. Such experiments will also be subject to the confinement and surface chemistry effects, as discussed above.

5.9. Underscreening and reentrant phenomena

The influence of increasing ionic strength on the stability of colloidal and macromolecular materials is well established. There have been several recent reports, however, of *reentrant* behaviour in these systems at high salt concentration, whereby colloidal or macromolecular materials redisperse/dissolve into solution. A selection of experimental reentrant work is shown in Fig. 8. In two examples of reentrant behaviour of silica nanoparticles (Fig. 8(a,b)) [61,62], nanoparticles are dispersed at low concentrations of salt (high transmittance of light), followed by flocculation (reduced transmittance), then increased transmittance again at higher salt concentration. It is noted this behaviour is not observed for some of the 1:1 electrolytes though. The

turn around point (or MEDL, assuming reentrance is driven by electrostatic interactions) in each of these cases is reduced when higher valence cations are used, in agreement with the SFB experiments of trivalent cations discussed in Section 4.1. Fig. 8(c) shows that the hydrodynamic radius of sodium polystyrene sulfonate (NaPSS) as a function of increasing concentration of various 1:n electrolytes is also an example of reentrant phenomena for several salts. This effect appears particularly enhanced for multivalent salts [277]. There are many additional examples of this phenomena in the literature; for instance, the solubility of DNA in the presence of tetravalent spermine [67], NaPSS in $LaCl_3$(aq) [299], chemically modified cellulose in various electrolytes [300], the force on micrometre sized particles in optical tweezers [301], coagulation of proteins [63,302] and in scattering of micellar solutions in deuterated water and deuterated DES [64]. Various other examples can be found where there is either an observed or predicted reversal of a behaviour with the origin likely to be electrostatic interactions [303–309]. Recent conductance measurements of ion-channel transport showed so-called biphasic behaviour [310], suggesting a possible common origin with reentrant phenomena. Further, another SFB work reported that a (neutral) poly(ethylene glycol) polymer brush extended further into $[C_2C_1im][TFSI]$, compared to water [311]. Correlations between colloidal nanocrystals dissolved in both molten salts or ILs was shown to extend well beyond the Debye length [312].

An analysis of existing polyelectrolyte literature by Liu et al. [313] suggested that the reentrant behaviour was due to the increase in the screening length that occurs at high salt concentrations, i.e. due to underscreening. Unfortunately, many of these experiments do not report or measure a value for λ, so it is unknown which, if any, of these reentrant systems exhibit anomalous underscreening. However, one notable simulation has suggested that normal underscreening resulted in reentrant behaviour of nanoparticles in monovalent salts [314]. Similarly, Robertson et al. [102] performed neutron scattering on a poly-(2-(methacryloyloxy)ethyl) trimethylammonium (PMETAC) polyelectrolyte polymer brush in the presence of 1:n electrolytes, see Fig. 8(d), and quantified the screening length (denoted λ_S^*). It was shown that it decreased initially, before increasing above ≈1 M ionic strength. Importantly, the underscreening observed was consistent with normal underscreening ($\xi \approx 2$). The critical micelle concentration (CMC) of the surfactant myristyltrimethylammonium bromide (MTAB) in aqueous electrolytes (Fig. 8(e)) also shows an initial decrease with salt concentration, followed by an increase above ≈2 M [61]. These results therefore highlight an as-yet underutilised route for elucidating the nature of underscreening. We believe that further study of soft matter and colloidal reentrant phenomena in highly concentration electrolytes (>1 M) should be an important area of focus in this field.

6. Summary and outlook

Despite enormous effort, there is still no universally accepted explanation of anomalous underscreening. The study of electrolytes and liquid structure is clearly far from complete, and continued exploration and discovery provides a unique opportunity for experiments, simulations and theoretical treatments to provide multifaceted insight into the origins of this intriguing phenomenon. Validation of recent theoretical treatments [78,138,172,199,238,276] can increasingly be achieved with an ever increasing computational capability [315,316] in conjunction with improved models of electronic structure and force-field sophistication (i.e. explicit polarisation [317,318] or inclusion of NQE [267,319,320]). Similarly, experimental techniques continue to deliver improved sensitivity and sophistication, as evidenced by X-ray photoelectron spectroscopy [321], and X-ray scattering [215, 216] approaches to imaging the electric double layer. Additionally, van Hove correlation functions [322], generated from inelastic X-ray or inelastic neutron scattering [48,49,323,324], or computed directly using atomistic MD [50,250,325], afford both spatial and temporal information of electrolyte structure, including ion-solvent correlations. Optical techniques such as dielectric relaxation spectroscopy [326–328], 2DIR [329–331], and other ultrafast/nonlinear techniques [51, 54,72,73,246,328,332–342] also promise to improve understanding of liquid spatial and temporal behaviour, as do prospective techniques such as X-ray SFB [343], which enable concurrent measurement of force and structural information.

Given that many techniques involve an interface, there is an imperative to establish a truly bulk measure of the screening length (to decouple surface effects). Measurements by Shelton [341] using hyper-Rayleigh scattering have shown excellent agreement with DH theory at low concentration, and this holds promise for bulk measurements of highly concentrated (>1 M) electrolytes. There has also been a recent study that mapped the electrostatic potential around ions [344] in a 1 M electrolyte. This approach provides a further avenue of bulk solution investigation. The principal opportunity facing computational researchers in this field is the use of electronic structure calculations to understand underscreening, considering the molecular nature of solvents themselves and the fact that electron density is non-local. We hope that this perspective encourages future work to unravel the complex nature of electrolytes and the origins of anomalous underscreening.

CRediT authorship contribution statement

Gareth R. Elliott: Writing – review & editing, Writing – original draft. **Kasimir P. Gregory:** Writing – review & editing. **Hayden Robertson:** Writing – review & editing. **Vincent S.J. Craig:** Writing – review & editing. **Grant B. Webber:** Writing – review & editing. **Erica J. Wanless:** Writing – review & editing. **Alister J. Page:** Writing – review & editing, Conceptualization.

Declaration of competing interest

The authors declare the following financial interests/personal relationships which may be considered as potential competing interests: Alister Page reports financial support was provided by Australian Research Council. If there are other authors, they declare that they have no known competing financial interests or personal relationships that could have appeared to influence the work reported in this paper.

Data availability

No data was used for the research described in the article.

Acknowledgements

The authors would like to thank Prof. Susan Perkin for providing Fig. 1. V.S.J.C, G.B.W, E.J.W, G.R. E. and A.J.P acknowledge funding from the Australian Research Council (ARC DP190100788, DP230102030). H.R thanks the Australian Government for providing a Research Training Scholarship and AINSE for a Postgraduate Research Award.

References

[1] A. Eftekhari, Potassium secondary cell based on Prussian blue cathode, J. Power Sources 126 (1–2) (2004) 221–228, http://dx.doi.org/10.1016/j.jpowsour.2003.08.007, URL https://linkinghub.elsevier.com/retrieve/pii/S0378775303008954.

[2] K. Xu, Electrolytes and interphases in Li-ion batteries and beyond, Chem. Rev. 114 (23) (2014) 11503–11618, http://dx.doi.org/10.1021/cr500003w, URL https://pubs.acs.org/doi/10.1021/cr500003w.

[3] D. Aurbach, Y. Talyosef, B. Markovsky, E. Markevich, E. Zinigrad, L. Asraf, J.S. Gnanaraj, H.-J. Kim, Design of electrolyte solutions for Li and Li-ion batteries: a review, Electrochim. Acta 50 (2–3) (2004) 247–254, http://dx.doi.org/10.1016/j.electacta.2004.01.090, URL https://linkinghub.elsevier.com/retrieve/pii/S0013468604006413.

[4] L. Fan, K. Lin, J. Wang, R. Ma, B. Lu, A nonaqueous potassium-based battery–supercapacitor hybrid device, Adv. Mater. 30 (20) (2018) 1800804, http://dx.doi.org/10.1002/adma.201800804, URL https://onlinelibrary.wiley.com/doi/abs/10.1002/adma.201800804.

[5] M. Winter, R.J. Brodd, What are batteries, fuel cells, and supercapacitors? Chem. Rev. 104 (10) (2004) 4245–4270, http://dx.doi.org/10.1021/cr020730k, URL http://dx.doi.org/10.1021/cr020730khttps://pubs.acs.org/doi/10.1021/cr020730k.

[6] J. Wei, Q. Wang, Hofmeister effect-aided assembly of enhanced hydrogel supercapacitor with excellent interfacial contact and reliability, Small Methods 3 (11) (2019) 1900558, http://dx.doi.org/10.1002/smtd.201900558.

[7] V. Artemov, The Electrodynamics of Water and Ice, in: Springer Series in Chemical Physics, vol. 124, Springer International Publishing, Cham, 2021, http://dx.doi.org/10.1007/978-3-030-72424-5, URL https://link.springer.com/10.1007/978-3-030-72424-5.

[8] V.S.J. Craig, B.W. Ninham, R.M. Pashley, Effect of electrolytes on bubble coalescence, Nature 364 (6435) (1993) 317–319, http://dx.doi.org/10.1038/364317a0, URL https://www.nature.com/articles/364317a0.

[9] C.L. Henry, V.S.J. Craig, The link between ion specific bubble coalescence and Hofmeister effects is the partitioning of ions within the interface, Langmuir 26 (9) (2010) 6478–6483, http://dx.doi.org/10.1021/la9039495.

[10] S. Wu, C. Zhu, Z. He, H. Xue, Q. Fan, Y. Song, J.S. Francisco, X.C. Zeng, J. Wang, Ion-specific ice recrystallization provides a facile approach for the fabrication of porous materials, Nature Commun. 8 (1) (2017) 15154, http://dx.doi.org/10.1038/ncomms15154, URL https://www.nature.com/articles/ncomms15154.

[11] N.K. Fageria, M.B. Filho, A. Moreira, C.M. Guimarães, Foliar fertilization of crop plants, J. Plant Nutr. 32 (6) (2009) 1044–1064, http://dx.doi.org/10.1080/01904160902872826, URL http://www.tandfonline.com/doi/abs/10.1080/01904160902872826.

[12] E.M. Wright, J.M. Diamond, Anion selectivity in biological systems, Physiol. Rev. 57 (1) (1977) 109–156, http://dx.doi.org/10.1152/physrev.1977.57.1.109, URL https://www.physiology.org/doi/10.1152/physrev.1977.57.1.109.

[13] P. Lo Nostro, B.W. Ninham, Hofmeister phenomena: An update on ion specificity in biology, Chem. Rev. 112 (4) (2012) 2286–2322, http://dx.doi.org/10.1021/cr200271j.

[14] H.I. Okur, J. Hladílková, K.B. Rembert, Y. Cho, J. Heyda, J. Dzubiella, P.S. Cremer, P. Jungwirth, Beyond the Hofmeister series: Ion-specific effects on proteins and their biological functions, J. Phys. Chem. B 121 (9) (2017) 1997–2014, http://dx.doi.org/10.1021/acs.jpcb.6b10797, URL https://pubs.acs.org/doi/10.1021/acs.jpcb.6b10797.

[15] B.W. Ninham, The biological/physical sciences divide, and the age of unreason, Substantia 1 (1) (2017) 7–24, http://dx.doi.org/10.13128/Substantia-6, URL http://riviste.fupress.net/index.php/subs/article/view/6.

[16] D.R. MacFarlane, A.L. Chong, M. Forsyth, M. Kar, R. Vijayaraghavan, A. Somers, J.M. Pringle, New dimensions in salt-solvent mixtures: A 4th evolution of ionic liquids, Faraday Discuss. 206 (2018) 9–28, http://dx.doi.org/10.1039/c7fd00189d.

[17] O. Borodin, J. Self, K.A. Persson, C. Wang, K. Xu, Uncharted waters: Superconcentrated electrolytes, Joule 4 (1) (2020) 69–100, http://dx.doi.org/10.1016/j.joule.2019.12.007.

[18] A.M. Fenton, R.K. Jha, B.J. Neyhouse, A.P. Kaur, D.A. Dailey, S.A. Odom, F.R. Brushett, On the challenges of materials and electrochemical characterization of concentrated electrolytes for redox flow batteries, J. Mater. Chem. A 10 (35) (2022) 17988–17999, http://dx.doi.org/10.1039/d2ta00690a.

[19] Y. Levin, Electrostatic correlations: From plasma to biology, Rep. Progr. Phys. 65 (11) (2002) 1577–1632, http://dx.doi.org/10.1088/0034-4885/65/11/201, arXiv:0207086.

[20] P. Yao, H. Yu, Z. Ding, Y. Liu, J. Lu, M. Lavorgna, J. Wu, X. Liu, Review on polymer-based composite electrolytes for lithium batteries, Front. Chem. 7 (August) (2019) 1–17, http://dx.doi.org/10.3389/fchem.2019.00522.

[21] K.S. Ngai, S. Ramesh, K. Ramesh, J.C. Juan, A review of polymer electrolytes: fundamental, approaches and applications, Ionics 22 (8) (2016) 1259–1279, http://dx.doi.org/10.1007/s11581-016-1756-4.

[22] D. Zhou, D. Shanmukaraj, A. Tkacheva, M. Armand, G. Wang, Polymer electrolytes for lithium-based batteries: Advances and prospects, Chem 5 (9) (2019) 2326–2352, http://dx.doi.org/10.1016/j.chempr.2019.05.009.

[23] V. Bocharova, A.P. Sokolov, Perspectives for polymer electrolytes: A view from fundamentals of ionic conductivity, Macromolecules 53 (11) (2020) 4141–4157, http://dx.doi.org/10.1021/acs.macromol.9b02742.

[24] N. Boaretto, L. Meabe, M. Martinez-Ibañez, M. Armand, H. Zhang, Review—Polymer electrolytes for rechargeable batteries: From nanocomposite to nanohybrid, J. Electrochem. Soc. 167 (7) (2020) 070524, http://dx.doi.org/10.1149/1945-7111/ab7221.

[25] K.H. Shen, L.M. Hall, Ion conductivity and correlations in model salt-doped polymers: Effects of interaction strength and concentration, Macromolecules 53 (10) (2020) 3655–3668, http://dx.doi.org/10.1021/acs.macromol.0c00216, arXiv:2001.09554.

[26] K.D. Fong, J. Self, B.D. McCloskey, K.A. Persson, Ion correlations and their impact on transport in polymer-based electrolytes, Macromolecules 54 (6) (2021) 2575–2591, http://dx.doi.org/10.1021/acs.macromol.0c02545.

[27] A.V. Dobrynin, Polyelectrolytes: On the doorsteps of the second century, Polymer 202 (May) (2020) 122714, http://dx.doi.org/10.1016/j.polymer.2020.122714.

[28] M. Muthukumar, 50Th anniversary perspective: A perspective on polyelectrolyte solutions, Macromolecules 50 (24) (2017) 9528–9560, http://dx.doi.org/10.1021/acs.macromol.7b01929.

[29] V.S. Meka, M.K. Sing, M.R. Pichika, S.R. Nali, V.R. Kolapalli, P. Kesharwani, A comprehensive review on polyelectrolyte complexes, Drug Discov. Today 22 (11) (2017) 1697–1706, http://dx.doi.org/10.1016/j.drudis.2017.06.008.

[30] E.N. Durmaz, S. Sahin, E. Virga, S. De Beer, L.C. De Smet, W.M. De Vos, Polyelectrolytes as building blocks for next-generation membranes with advanced functionalities, ACS Appl. Polym. Mater. 3 (9) (2021) 4347–4374, http://dx.doi.org/10.1021/acsapm.1c00654.

[31] B.B. Hansen, S. Spittle, B. Chen, D. Poe, Y. Zhang, J.M. Klein, A. Horton, L. Adhikari, T. Zelovich, B.W. Doherty, B. Gurkan, E.J. Maginn, A. Ragauskas, M. Dadmun, T.A. Zawodzinski, G.A. Baker, M.E. Tuckerman, R.F. Savinell, J.R. Sangoro, Deep eutectic solvents: A review of fundamentals and applications, Chem. Rev. 121 (3) (2021) 1232–1285, http://dx.doi.org/10.1021/acs.chemrev.0c00385.

[32] A.P. Abbott, K.J. Edler, A.J. Page, Deep eutectic solvents—The vital link between ionic liquids and ionic solutions, J. Chem. Phys. 155 (15) (2021) http://dx.doi.org/10.1063/5.0072268.

[33] R. Hayes, G.G. Warr, R. Atkin, Structure and nanostructure in ionic liquids, Chem. Rev. 115 (13) (2015) 6357–6426, http://dx.doi.org/10.1021/cr500411q.

[34] R. Roper, M. Harkema, P. Sabharwall, C. Riddle, B. Chisholm, B. Day, P. Marotta, Molten salt for advanced energy applications: A review, Ann. Nucl. Energy 169 (2022) 108924, http://dx.doi.org/10.1016/j.anucene.2021.108924.

[35] K.P. Gregory, G.R. Elliott, H. Robertson, A. Kumar, E.J. Wanless, G.B. Webber, V.S. Craig, G.G. Andersson, A.J. Page, Understanding specific ion effects and the Hofmeister series, Phys. Chem. Chem. Phys. 24 (21) (2022) 12682–12718, http://dx.doi.org/10.1039/d2cp00847e.

[36] K.P. Gregory, E.J. Wanless, G.B. Webber, V.S.J. Craig, A.J. Page, The electrostatic origins of specific ion effects: quantifying the Hofmeister series for anions, Chem. Sci. (2021) 21–23, http://dx.doi.org/10.1039/d1sc03568a.

[37] V. Mazzini, G. Liu, V.S. Craig, Probing the Hofmeister series beyond water: Specific-ion effects in non-aqueous solvents, J. Chem. Phys. 148 (22) (2018) http://dx.doi.org/10.1063/1.5017278.

[38] R.A. Miranda-Quintana, J. Smiatek, Specific ion effects in different media: Current status and future challenges, J. Phys. Chem. B 125 (51) (2021) 13840–13849, http://dx.doi.org/10.1021/acs.jpcb.1c07957.

[39] T. Bourke, K.P. Gregory, A.J. Page, Hofmeister effects influence bulk nanostructure in a protic ionic liquid, J. Colloid Interface Sci. 645 (January) (2023) 420–428, http://dx.doi.org/10.1016/j.jcis.2023.04.052.

[40] V. Mazzini, V.S. Craig, What is the fundamental ion-specific series for anions and cations? ion specificity in standard partial molar volumes of electrolytes and electrostriction in water and non-aqueous solvents, Chem. Sci. 8 (10) (2017) 7052–7065, http://dx.doi.org/10.1039/c7sc02691a.

[41] S. Perkin, 2023. Private Communication.

[42] S.M. Kathmann, Electric fields and potentials in condensed phases, Phys. Chem. Chem. Phys. 23 (41) (2021) 23836–23849, http://dx.doi.org/10.1039/d1cp03571a.

[43] R. Buchner, G.T. Hefter, P.M. May, Dielectric relaxation of aqueous NaCl solutions, J. Phys. Chem. A 103 (1) (1999) 8–9, http://dx.doi.org/10.1021/jp982977k.

[44] D.A. Turton, J. Hunger, G. Hefter, R. Buchner, K. Wynne, Glasslike behavior in aqueous electrolyte solutions, J. Chem. Phys. 128 (16) (2008) http://dx.doi.org/10.1063/1.2906132.

[45] R. Buchner, G. Hefter, Interactions and dynamics in electrolyte solutions by dielectric spectroscopy, Phys. Chem. Chem. Phys. 11 (40) (2009) 8984–8999, http://dx.doi.org/10.1039/b906555p.

[46] W. Wachter, W. Kunz, R. Buchner, G. Hefter, Is there an anionic Hofmeister effect on water dynamics? Dielectric spectroscopy of aqueous solutions of NaBr, NaI, $NaNO_3$, $NaClO_4$, and NaSCN, J. Phys. Chem. A 109 (39) (2005) 8675–8683, http://dx.doi.org/10.1021/jp053299m.

[47] P. Luo, Y. Zhai, E. Senses, E. Mamontov, G. Xu, Y. Zhyang, A. Faraone, Influence of kosmotrope and chaotrope salts on water structural relaxation, J. Phys. Chem. Lett. (2020) 8970–8975, http://dx.doi.org/10.1021/acs.jpclett.0c02619.

[48] Y. Shinohara, W. Dmowski, T. Iwashita, D. Ishikawa, A.Q. Baron, T. Egami, Local correlated motions in aqueous solution of sodium chloride, Phys. Rev. Mater. 3 (6) (2019) 65604, http://dx.doi.org/10.1103/PhysRevMaterials.3.065604.

[49] Y. Shinohara, R. Matsumoto, M.W. Thompson, C.W. Ryu, W. Dmowski, T. Iwashita, D. Ishikawa, A.Q. Baron, P.T. Cummings, T. Egami, Identifying water-anion correlated motion in aqueous solutions through van hove functions, J. Phys. Chem. Lett. 10 (22) (2019) 7119–7125, http://dx.doi.org/10.1021/acs.jpclett.9b02891.

[50] R. Khanal, S. Irle, Quantum chemical investigation of the effect of alkali metal ions on the dynamic structure of water in aqueous solutions, RSC Adv. 12 (39) (2022) 25500–25510, http://dx.doi.org/10.1039/D2RA04563J, URL http://xlink.rsc.org/?DOI=D2RA04563J.

[51] V. Balos, N.K. Kaliannan, H. Elgabarty, M. Wolf, T.D. Kühne, M. Sajadi, Time-resolved terahertz–Raman spectroscopy reveals that cations and anions distinctly modify intermolecular interactions of water, Nature Chem. 14 (9) (2022) 1031–1037, http://dx.doi.org/10.1038/s41557-022-00977-2.

[52] E. Pluhařová, D. Laage, P. Jungwirth, Size and origins of long-range orientational water correlations in dilute aqueous salt solutions, J. Phys. Chem. Lett. 8 (9) (2017) 2031–2035, http://dx.doi.org/10.1021/acs.jpclett.7b00727.

[53] A. Onuki, Long-range correlations of polarization and number densities in dilute electrolytes, J. Chem. Phys. 153 (23) (2020) 234501, http://dx.doi.org/10.1063/5.0030763.

[54] Y. Chen, H.I. Okur, N. Gomopoulos, C. Macias-Romero, P.S. Cremer, P.B. Petersen, G. Tocci, D.M. Wilkins, C. Liang, M. Ceriotti, S. Roke, Electrolytes induce long-range orientational order and free energy changes in the H-bond network of bulk water, Sci. Adv. 2 (4) (2016) 1–9, http://dx.doi.org/10.1126/sciadv.1501891.

[55] D.P. Shelton, Water-water correlations in electrolyte solutions probed by hyper-Rayleigh scattering, J. Chem. Phys. 147 (21) (2017) http://dx.doi.org/10.1063/1.4998589.

[56] J.-P. Hansen, I.R. McDonald, Theory of Simple Liquids : With Applications to Soft Matter, fourth ed., Elsevier Science & Technology, San Diego, UNITED KINGDOM, 2013, p. 404, URL https://www.sciencedirect.com/book/9780123870322/theory-of-simple-liquids.

[57] P. Debye, E. Hückel, Zur theorie der elektrolyte, Phys. Z. 9 (1923) 185–206.

[58] R. Kjellander, Statistical Mechanics of Liquids and Solutions, CRC Press, 2019, http://dx.doi.org/10.1201/9780429194368.

[59] D.A. McQuarrie, Statistical Mechanics, in: G - Reference,Information and Interdisciplinary Subjects Series, University Science Books, 2000.

[60] G. Livadiotis, Chapter 5 - basic plasma parameters described by kappa distributions, in: G. Livadiotis (Ed.), Kappa Distributions, Elsevier, 2017, pp. 249–312, http://dx.doi.org/10.1016/B978-0-12-804638-8.00005-X, URL https://www.sciencedirect.com/science/article/pii/B978012804638800005X.

[61] H. Yuan, W. Deng, X. Zhu, G. Liu, V.S.J. Craig, Colloidal systems in concentrated electrolyte solutions exhibit re-entrant long-range electrostatic interactions due to underscreening, Langmuir 38 (19) (2022) 6164–6173, http://dx.doi.org/10.1021/acs.langmuir.2c00519, URL https://pubs.acs.org/doi/10.1021/acs.langmuir.2c00519.

[62] S. Kumar, I. Yadav, S. Abbas, V.K. Aswal, J. Kohlbrecher, Interactions in reentrant phase behavior of a charged nanoparticle solution by multivalent ions, Phys. Rev. E 96 (6) (2017) 2–6, http://dx.doi.org/10.1103/PhysRevE.96.060602.

[63] S. Kumar, D. Ray, S. Abbas, D. Saha, V.K. Aswal, J. Kohlbrecher, Reentrant phase behavior of nanoparticle solutions probed by small-angle scattering, Curr. Opin. Colloid Interface Sci. 42 (2019) 17–32, http://dx.doi.org/10.1016/j.cocis.2019.02.010.

[64] A. Sanchez-Fernandez, A.J. Jackson, S.F. Prévost, J.J. Doutch, K.J. Edler, Long-range electrostatic colloidal interactions and specific ion effects in deep eutectic solvents, J. Am. Chem. Soc. (2021) http://dx.doi.org/10.1021/jacs.1c04781.

[65] H. Träuble, H. Eibl, Electrostatic effects on lipid phase transitions: Membrane structure and ionic environment, Proc. Natl. Acad. Sci. 71 (1) (1974) 214–219, http://dx.doi.org/10.1073/pnas.71.1.214, URL https://doi.org/10.1073/pnas.71.1.214https://pnas.org/doi/full/10.1073/pnas.71.1.214.

[66] Y. Zhang, P.S. Cremer, The inverse and direct Hofmeister series for lysozyme, Proc. Natl. Acad. Sci. USA 106 (36) (2009) 15249–15253, http://dx.doi.org/10.1073/pnas.0907616106.

[67] E. Raspaud, M. Olvera De La Cruz, J.L. Sikorav, F. Livolant, Precipitation of DNA by polyamines: A polyelectrolyte behaviour, Biophys. J. 74 (1) (1998) 381–393, http://dx.doi.org/10.1016/S0006-3495(98)77795-1.

[68] S.E. Seo, M. Girard, M.O. de la Cruz, C.A. Mirkin, The importance of salt-enhanced electrostatic repulsion in colloidal crystal engineering with DNA, ACS Cent. Sci. 5 (1) (2019) 186–191, http://dx.doi.org/10.1021/acscentsci.8b00826.

[69] G. Feng, M. Chen, S. Bi, Z.A. Goodwin, E.B. Postnikov, N. Brilliantov, M. Urbakh, A.A. Kornyshev, Free and bound states of ions in ionic liquids, conductivity, and underscreening paradox, Phys. Rev. X 9 (2) (2019) 21024, http://dx.doi.org/10.1103/PhysRevX.9.021024.

[70] Y. Avni, R.M. Adar, D. Andelman, H. Orland, Conductivity of concentrated electrolytes, Phys. Rev. Lett. 128 (9) (2022) 98002, http://dx.doi.org/10.1103/PhysRevLett.128.098002, arXiv:2110.07008.

[71] Y. Avni, D. Andelman, H. Orland, Conductance of concentrated electrolytes: Multivalency and the wien effect, J. Chem. Phys. 157 (15) (2022) http://dx.doi.org/10.1063/5.0111645, arXiv:2207.10116. URL http://arxiv.org/abs/2207.10116https://pubs.aip.org/jcp/article/157/15/154502/2842016/Conductance-of-concentrated-electrolytes.

[72] V. Artemov, A. Ryzhov, H. Ouerdane, K.J. Stevenson, Ionization difference between weak and strong electrolytes as perturbed by conductivity spectra analysis, J. Phys. Chem. B (2022) http://dx.doi.org/10.1021/acs.jpcb.2c06713.

[73] V. Balos, S. Imoto, R.R. Netz, M. Bonn, D.J. Bonthuis, Y. Nagata, J. Hunger, Macroscopic conductivity of aqueous electrolyte solutions scales with ultrafast microscopic ion motions, Nature Commun. 11 (1) (2020) 1–8, http://dx.doi.org/10.1038/s41467-020-15450-2.

[74] Z.A. Goodwin, A.A. Kornyshev, Underscreening, overscreening and double-layer capacitance, Electrochem. Commun. 82 (June) (2017) 129–133, http://dx.doi.org/10.1016/j.elecom.2017.07.008.

[75] S. Angizi, L. Hong, X. Huang, P.R. Selvaganapathy, P. Kruse, Graphene versus concentrated aqueous electrolytes: the role of the electrochemical double layer in determining the screening length of an electrolyte, NPJ 2D Mater. Appl. 7 (1) (2023) 67, http://dx.doi.org/10.1038/s41699-023-00431-y, URL https://www.nature.com/articles/s41699-023-00431-y.

[76] I.C. Bourg, S.S. Lee, P. Fenter, C. Tournassat, Stern layer structure and energetics at mica-water interfaces, J. Phys. Chem. C 121 (17) (2017) 9402–9412, http://dx.doi.org/10.1021/acs.jpcc.7b01828.

[77] M.A. Gebbie, B. Liu, W. Guo, S.R. Anderson, S.G. Johnstone, Linking electric double layer formation to electrocatalytic activity, ACS Catal. (2023) 16222–16239, http://dx.doi.org/10.1021/acscatal.3c04255.

[78] A. Härtel, M. Bültmann, F. Coupette, Anomalous underscreening in the restricted primitive model, Phys. Rev. Lett. 130 (10) (2022) 108202, http://dx.doi.org/10.1103/PhysRevLett.130.108202, arXiv:2209.03486. URL http://arxiv.org/abs/2209.03486.

[79] A.M. Smith, A.A. Lee, S. Perkin, The electrostatic screening length in concentrated electrolytes increases with concentration, J. Phys. Chem. Lett. 7 (12) (2016) 2157–2163, http://dx.doi.org/10.1021/acs.jpclett.6b00867.

[80] R.M. Pashley, J.N. Israelachvili, Molecular layering of water in thin films between mica surfaces and its relation to hydration forces, J. Colloid Interface Sci. 101 (2) (1984) 511–523, http://dx.doi.org/10.1016/0021-9797(84)90063-8.

[81] T. Baimpos, B.R. Shrestha, S. Raman, M. Valtiner, Effect of interfacial ion structuring on range and magnitude of electric double layer, hydration, and adhesive interactions between mica surfaces in 0.05-3 M Li^+ and Cs^+ electrolyte solutions, Langmuir 30 (15) (2014) 4322–4332, http://dx.doi.org/10.1021/la500288w.

[82] C. Fung, Static and Dynamic Behaviour of Ionic Liquid Films Studied with the Surface Force Apparatus (Ph.D. thesis), University of South Australia, 2022.

[83] M.A. Gebbie, M. Valtiner, X. Banquy, E.T. Fox, W.A. Henderson, J.N. Israelachvili, Ionic liquids behave as dilute electrolyte solutions, Proc. Natl. Acad. Sci. USA 110 (24) (2013) 9674–9679, http://dx.doi.org/10.1073/pnas.1307871110.

[84] C. Fung, S. Perkin, Structure and anomalous underscreening in ethylammonium nitrate solutions confined between two mica surfaces, Faraday Discuss. (2023) http://dx.doi.org/10.1039/D3FD00042G, URL http://pubs.rsc.org/en/Content/ArticleLanding/2023/FD/D3FD00042G.

[85] M. Han, R.M. Espinosa-Marzal, Electroviscous retardation of the squeeze out of nanoconfined ionic liquids, J. Phys. Chem. C 122 (37) (2018) 21344–21355, http://dx.doi.org/10.1021/acs.jpcc.8b04778.

[86] R.M. Espinosa-Marzal, A. Arcifa, A. Rossi, N.D. Spencer, Microslips to "avalanches" in confined, molecular layers of ionic liquids, J. Phys. Chem. Lett. 5 (1) (2014) 179–184, http://dx.doi.org/10.1021/jz402451v.

[87] M. Han, H. Kim, C. Leal, M. Negrito, J.D. Batteas, R.M. Espinosa-Marzal, Insight into the electrical double layer of ionic liquids revealed through its temporal evolution, Adv. Mater. Interfaces 7 (24) (2020) 1–10, http://dx.doi.org/10.1002/admi.202001313.

[88] A.A. Lee, C.S. Perez-Martinez, A.M. Smith, S. Perkin, Underscreening in concentrated electrolytes, Faraday Discuss. 199 (2017) 239–259, http://dx.doi.org/10.1039/c6fd00250a, arXiv:1701.08151.

[89] A.A. Lee, C.S. Perez-Martinez, A.M. Smith, S. Perkin, Scaling analysis of the screening length in concentrated electrolytes, Phys. Rev. Lett. 119 (2) (2017) 1–5, http://dx.doi.org/10.1103/PhysRevLett.119.026002, arXiv:1706.02221.

[90] V. Adibnia, M. Mirbagheri, P.-L. Latreille, G. De Crescenzo, D. Rochefort, X. Banquy, Interfacial forces across ionic liquid solutions: Effects of ion concentration and water domains, Langmuir 35 (48) (2019) 15585–15591, http://dx.doi.org/10.1021/acs.langmuir.9b02011, URL https://pubs.acs.org/doi/10.1021/acs.langmuir.9b02011.

[91] R.M. Pashley, Forces between mica surfaces in La3+ and Cr3+ electrolyte solutions, J. Colloid Interface Sci. 102 (1) (1984) 23–35, http://dx.doi.org/10.1016/0021-9797(84)90197-8.

[92] Q. Tan, G. Zhao, Y. Qiu, Y. Kan, Z. Ni, Y. Chen, Experimental observation of the ion-ion correlation effects on charge inversion and strong adhesion between mica surfaces in aqueous electrolyte solutions, Langmuir 30 (36) (2014) 10845–10854, http://dx.doi.org/10.1021/la5024357.

[93] T. Han, W. Cao, Z. Xu, V. Adibnia, M. Olgiati, M. Valtiner, L. Ma, C. Zhang, M. Ma, J. Luo, X. Banquy, Hydration layer structure modulates superlubrication by trivalent la 3+ electrolytes, Sci. Adv. 9 (28) (2023) 1–12, http://dx.doi.org/10.1126/sciadv.adf3902, URL https://www.science.org/doi/10.1126/sciadv.adf3902.

[94] J.E. Hallett, H.J. Hayler, S. Perkin, Nanolubrication in deep eutectic solvents, Phys. Chem. Chem. Phys. 22 (36) (2020) 20253–20264, http://dx.doi.org/10.1039/d0cp03787g.

[95] J.E. Hallett, K.J. Agg, S. Perkin, Zwitterions fine-tune interactions in electrolyte solutions, Proc. Natl. Acad. Sci. 120 (8) (2023) 1–7, http://dx.doi.org/10.1073/pnas.2215585120, URL https://pnas.org/doi/10.1073/pnas.2215585120.

[96] T.S. Groves, C.S. Perez-Martinez, R. Lhermerout, S. Perkin, Surface forces and structure in a water-in-salt electrolyte, J. Phys. Chem. Lett. 12 (6) (2021) 1702–1707, http://dx.doi.org/10.1021/acs.jpclett.0c03718.

[97] M.M. Kohonen, M.E. Karaman, R.M. Pashley, Debye length in multivalent electrolyte solutions, Langmuir 16 (13) (2000) 5749–5753, http://dx.doi.org/10.1021/la991621c.

[98] V. Adibnia, B.R. Shrestha, M. Mirbagheri, F. Murschel, G. De Crescenzo, X. Banquy, Electrostatic screening length in “soft” electrolyte solutions, ACS Macro Lett. 8 (8) (2019) 1017–1021, http://dx.doi.org/10.1021/acsmacrolett.9b00437.

[99] S. Kumar, P. Cats, M.B. Alotaibi, S.C. Ayirala, A.A. Yousef, R. Van Roij, I. Siretanu, F. Mugele, Absence of anomalous underscreening in highly concentrated aqueous electrolytes confined between smooth silica surfaces, J. Colloid Interface Sci. 622 (2022) 819–827, http://dx.doi.org/10.1016/j.jcis.2022.05.004, arXiv:2201.08667. URL http://arxiv.org/abs/2201.08667.

[100] A.M. Smith, P. Maroni, G. Trefalt, M. Borkovec, Unexpectedly large decay lengths of double-layer forces in solutions of symmetric, multivalent electrolytes, J. Phys. Chem. B 123 (7) (2019) 1733–1740, http://dx.doi.org/10.1021/acs.jpcb.8b12246.

[101] P. Gaddam, W. Ducker, Electrostatic screening length in concentrated salt solutions, Langmuir 35 (17) (2019) 5719–5727, http://dx.doi.org/10.1021/acs.langmuir.9b00375.

[102] H. Robertson, G.R. Elliott, A.R.J. Nelson, A.P. Le Brun, G.B. Webber, S.W. Prescott, V.S.J. Craig, E.J. Wanless, J.D. Willott, Underscreening in concentrated electrolytes: re-entrant swelling in polyelectrolyte brushes, Phys. Chem. Chem. Phys. (2023) http://dx.doi.org/10.1039/D3CP02206D, DOI: 10.5281/zenodo.7743201. URL doi.org/10.5281/zenodo.7743201http://xlink.rsc.org/?DOI=D3CP02206D.

[103] S.W. Coles, C. Park, R. Nikam, M. Kanduč, J. Dzubiella, B. Rotenberg, Correlation length in concentrated electrolytes: Insights from all-atom molecular dynamics simulations, J. Phys. Chem. B 124 (9) (2020) 1778–1786, http://dx.doi.org/10.1021/acs.jpcb.9b10542.

[104] J. Zeman, S. Kondrat, C. Holm, Bulk ionic screening lengths from extremely large-scale molecular dynamics simulations, Chem. Commun. 56 (100) (2020) 15635–15638, http://dx.doi.org/10.1039/d0cc05023g.

[105] M. Vranes, S. Dozic, V. Djeric, S. Gadzuric, Physicochemical characterization of 1-butyl-3-methylimidazolium and 1-butyl-1-methylpyrrolidinium bis(trifluoromethylsulfonyl)imide, J. Chem. Eng. Data 57 (4) (2012) 1072–1077, http://dx.doi.org/10.1021/je2010837, URL https://pubs.acs.org/doi/10.1021/je2010837.

[106] D.J. Griffiths, Introduction to Electrodynamics, fourth ed., Pearson, 2013.

[107] G.M. Silva, X. Liang, G.M. Kontogeorgis, Investigation of the limits of the linearized Poisson-Boltzmann equation, J. Phys. Chem. B 126 (22) (2022) 4112–4131, http://dx.doi.org/10.1021/acs.jpcb.2c02758.

[108] R. Kjellander, Nonlocal electrostatics in ionic liquids: The key to an understanding of the screening decay length and screened interactions, J. Chem. Phys. 145 (12) (2016) http://dx.doi.org/10.1063/1.4962756.

[109] H. Helmholtz, Ueber einige gesetze der vertheilung elektrischer ströme in körperlichen leitern mit anwendung auf die thierisch-elektrischen versuche, Ann. Phys. Chem. 165 (6) (1853) 211–233, http://dx.doi.org/10.1002/andp.18531650603, URL https://doi.org/10.1002/andp.18531650603https://onlinelibrary.wiley.com/doi/10.1002/andp.18531650603.

[110] H. Helmholtz, Studien über electrische grenzschichten, Ann. Phys. Chem. 243 (7) (1879) 337–382, http://dx.doi.org/10.1002/andp.18792430702, URL https://onlinelibrary.wiley.com/doi/abs/10.1002/andp.18792430702https://onlinelibrary.wiley.com/doi/10.1002/andp.18792430702.

[111] O. Stern, Zur theorie der elektrolytischen doppelschicht, Z. Elektrochem. Angew. Phys. Chem. 30 (21–22) (1924) 508–516, http://dx.doi.org/10.1002/bbpc.192400182, URL https://onlinelibrary.wiley.com/doi/abs/10.1002/bbpc.192400182https://onlinelibrary.wiley.com/doi/10.1002/bbpc.192400182.

[112] D.C. Grahame, The electrical double layer and the theory of electrocapillarity, Chem. Rev. 41 (3) (1947) 441–501, http://dx.doi.org/10.1021/cr60130a002, URL https://doi.org/10.1021/cr60130a002https://pubs.acs.org/doi/abs/10.1021/cr60130a002.

[113] M. Gouy, Sur la constitution de la charge électrique à la surface d’un électrolyte, J. Phys. Théor. Appl. 9 (1) (1910) 457–468, http://dx.doi.org/10.1051/jphystap:019100090045700, URL http://www.edpsciences.org/10.1051/jphystap:019100090045700.

[114] D.L. Chapman, LI. A contribution to the theory of electrocapillarity, Lond. Edinb. Dublin Philos. Mag. J. Sci. 25 (148) (1913) 475–481, http://dx.doi.org/10.1080/14786440408634187.

[115] B. Rehl, E. Ma, S. Parshotam, E.L. Dewalt-Kerian, T. Liu, F.M. Geiger, J.M. Gibbs, Water structure in the electrical double layer and the contributions to the total interfacial potential at different surface charge densities, J. Am. Chem. Soc. 144 (36) (2022) 16338–16349, http://dx.doi.org/10.1021/jacs.2c01830.

[116] G. Gonella, E.H. Backus, Y. Nagata, D.J. Bonthuis, P. Loche, A. Schlaich, R.R. Netz, A. Kühnle, I.T. McCrum, M.T. Koper, M. Wolf, B. Winter, G. Meijer, R.K. Campen, M. Bonn, Water at charged interfaces, Nature Rev. Chem. 5 (7) (2021) 466–485, http://dx.doi.org/10.1038/s41570-021-00293-2.

[117] J. Wu, Understanding the electric double-layer structure, capacitance, and charging dynamics, Chem. Rev. 122 (12) (2022) 10821–10859, http://dx.doi.org/10.1021/acs.chemrev.2c00097.

[118] L. Onsager, R.M. Fuoss, Irreversible processes in electrolytes. Diffusion, conductance and viscous flow in arbitrary mixtures of strong electrolytes, J. Phys. Chem. 36 (11) (1932) 2689–2778, http://dx.doi.org/10.1021/j150341a001.

[119] L. Onsager, S.K. Kim, The relaxation effects in mixed strong electrolytes, J. Phys. Chem. 61 (2) (1957) 215–229, http://dx.doi.org/10.1021/j150548a016.

[120] M.-S. Chen, L. Onsager, The generalized conductance equation, J. Phys. Chem. 81 (21) (1977) 2017–2021, http://dx.doi.org/10.1021/j100536a013.

[121] J.G. Kirkwood, J.C. Poirier, The statistical mechanical basis of the Debye-Hückel theory of strong electrolytes, J. Phys. Chem. 58 (8) (1954) 591–596, http://dx.doi.org/10.1021/j150518a004.

[122] N. Gavish, D. Elad, A. Yochelis, From solvent-free to dilute electrolytes: Essential components for a continuum theory, J. Phys. Chem. Lett. 9 (1) (2018) 36–42, http://dx.doi.org/10.1021/acs.jpclett.7b03048, arXiv:1707.06940.

[123] E.A. Guggenheim, J.C. Turgeon, Specific interaction of ions, Trans. Faraday Soc. 51 (1955) 747, http://dx.doi.org/10.1039/tf9555100747, URL http://xlink.rsc.org/?DOI=tf9555100747.

[124] P. Sipos, Application of the specific ion interaction theory (SIT) for the ionic products of aqueous electrolyte solutions of very high concentrations, J. Mol. Liq. 143 (1) (2008) 13–16, http://dx.doi.org/10.1016/j.molliq.2008.04.003, URL https://linkinghub.elsevier.com/retrieve/pii/S0167732208000676.

[125] K.S. Pitzer, Thermodynamics of electrolytes. I. Theoretical basis and general equations, J. Phys. Chem. 77 (2) (1973) 268–277, http://dx.doi.org/10.1021/j100621a026.

[126] K.S. Pitzer, Activity coefficients in electrolyte solutions, 2018, http://dx.doi.org/10.1201/9781351069472.

[127] G.M. Kontogeorgis, B. Maribo-Mogensen, K. Thomsen, The Debye-Hückel theory and its importance in modeling electrolyte solutions, Fluid Phase Equilib. 462 (2018) 130–152, http://dx.doi.org/10.1016/j.fluid.2018.01.004.

[128] G.M. Silva, X. Liang, G.M. Kontogeorgis, On the derivations of the Debye–Hückel equations, Mol. Phys. 120 (10) (2022) http://dx.doi.org/10.1080/00268976.2022.2064353.

[129] R. Kjellander, D.J. Mitchell, An exact but linear and Poisson-Boltzmann-like theory for electrolytes and colloid dispersions in the primitive model, Chem. Phys. Lett. 200 (1–2) (1992) 76–82, http://dx.doi.org/10.1016/0009-2614(92)87048-T.

[130] J. Ulander, R. Kjellander, Screening and asymptotic decay of pair distributions in asymmetric electrolytes, J. Chem. Phys. 109 (21) (1998) 9508–9522, http://dx.doi.org/10.1063/1.477613.

[131] R. Kjellander, D.J. Mitchell, Dressed-ion theory for electrolyte solutions: A Debye-Hückel-like reformulation of the exact theory for the primitive model, J. Chem. Phys. 101 (1) (1994) 603–626, http://dx.doi.org/10.1063/1.468116.

[132] R. Ramirez, R. Kjellander, Effective multipoles and Yukawa electrostatics in dressed molecule theory, J. Chem. Phys. 125 (14) (2006) http://dx.doi.org/10.1063/1.2355486.

[133] R. Kjellander, R. Ramirez, Yukawa multipole electrostatics and nontrivial coupling between electrostatic and dispersion interactions in electrolytes, J. Phys. Condens. Matter 20 (49) (2008) http://dx.doi.org/10.1088/0953-8984/20/49/494209.

[134] R. Ramirez, R. Kjellander, Dressed molecule theory for liquids and solutions: An exact charge renormalization formalism for molecules with arbitrary charge distributions, J. Chem. Phys. 119 (21) (2003) 11380–11395, http://dx.doi.org/10.1063/1.1623179, URL http://aip.scitation.org/doi/10.1063/1.1623179.

[135] R. Kjellander, Decay behavior of screened electrostatic surface forces in ionic liquids: The vital role of non-local electrostatics, Phys. Chem. Chem. Phys. 18 (28) (2016) 18985–19000, http://dx.doi.org/10.1039/c6cp02418a.

[136] R. Kjellander, The intimate relationship between the dielectric response and the decay of intermolecular correlations and surface forces in electrolytes, Soft Matter 15 (29) (2019) 5866–5895, http://dx.doi.org/10.1039/c9sm00712a.

[137] R. Kjellander, Statistical Mechanics of Liquids and Solutions, CRC Press, 2019, pp. 299–302, http://dx.doi.org/10.1201/9780429194368.

[138] R. Kjellander, A multiple decay-length extension of the Debye-Hückel theory: To achieve high accuracy also for concentrated solutions and explain underscreening in dilute symmetric electrolytes, Phys. Chem. Chem. Phys. 22 (41) (2020) 23952–23985, http://dx.doi.org/10.1039/d0cp02742a.

[139] R. Kjellander, Statistical Mechanics of Liquids and Solutions, CRC Press, 2019, pp. 303–304, http://dx.doi.org/10.1201/9780429194368.

[140] J.G. Kirkwood, Statistical mechanics of liquid solutions, Chem. Rev. 19 (3) (1936) 275–307, http://dx.doi.org/10.1021/cr60064a007.

[141] L.M. Varela, M. García, V. Mosquera, Exact mean-field theory of ionic solutions: Non-debye screening, Phys. Rep. 382 (1–2) (2003) 1–111, http://dx.doi.org/10.1016/S0370-1573(03)00210-2.

[142] H. Jäger, A. Schlaich, J. Yang, C. Lian, S. Kondrat, C. Holm, A screening of results on the decay length in concentrated electrolytes, Faraday Discuss. (2023) http://dx.doi.org/10.1039/D3FD00043E, URL http://xlink.rsc.org/?DOI=D3FD00043E.

[143] R.M. Espinosa-Marzal, Z.A.H. Goodwin, X. Zhang, Q. Zheng, Colloidal interactions in ionic liquids—The electrical double layer inferred from ion layering and aggregation, in: One Hundred Years of Colloid Symposia: Looking Back and Looking Forward, Part 7 - Colloidal Interactions in Ionic Liquids—the Electrical Double Layer Inferred from Ion Layering and Aggregation, American Chemical Society, 2023, pp. 123–148, http://dx.doi.org/10.1021/bk-2023-1457.ch007, URL https://pubs.acs.org/doi/abs/10.1021/bk-2023-1457.ch007.

[144] R.J. Leote De Carvalho, R. Evans, The decay of correlations in ionic fluids, Mol. Phys. 83 (4) (1994) 619–654, http://dx.doi.org/10.1080/00268979400101491.

[145] R. Evans, R.J. Leote De Carvalho, J.R. Henderson, D.C. Hoyle, Asymptotic decay of correlations in liquids and their mixtures, J. Chem. Phys. 100 (1) (1994) 591–603, http://dx.doi.org/10.1063/1.466920.

[146] P. Attard, Asymptotic analysis of primitive model electrolytes and the electrical double layer, Phys. Rev. E 48 (5) (1993) 3604–3621, http://dx.doi.org/10.1103/PhysRevE.48.3604.

[147] L. Ornstein, F. Zernike, Accidental deviations of density and opalescence at the critical point of a single substance, Proc. Akad. Sci. (Amsterdam) XVII (September) (1914) 793–806, URL http://www.dwc.knaw.nl/DL/publications/PU00012727.pdf.

[148] M.Z. Bazant, B.D. Storey, A.A. Kornyshev, Double layer in ionic liquids: Overscreening versus crowding, Phys. Rev. Lett. 106 (4) (2011) 6–9, http://dx.doi.org/10.1103/PhysRevLett.106.046102, arXiv:1010.3490.

[149] H. Frusawa, Electric-field-induced oscillations in ionic fluids: a unified formulation of modified Poisson–Nernst–Planck models and its relevance to correlation function analysis, Soft Matter 18 (22) (2022) 4280–4304, http://dx.doi.org/10.1039/D1SM01811F, arXiv:2203.15428.

[150] N.B. Ludwig, K. Dasbiswas, D.V. Talapin, S. Vaikuntanathan, Describing screening in dense ionic fluids with a charge-frustrated ising model, J. Chem. Phys. 149 (16) (2018) http://dx.doi.org/10.1063/1.5043410, arXiv:1810.00918.

[151] R.M. Adar, S.A. Safran, H. Diamant, D. Andelman, Screening length for finite-size ions in concentrated electrolytes, Phys. Rev. E 100 (4) (2019) 42615, http://dx.doi.org/10.1103/PhysRevE.100.042615, arXiv:1812.07217.

[152] B. Rotenberg, O. Bernard, J.P. Hansen, Underscreening in ionic liquids: A first principles analysis, J. Phys. Condens. Matter 30 (5) (2018) http://dx.doi.org/10.1088/1361-648X/aaa3ac.

[153] A. Grisafi, F. Grasselli, Effect of a temperature gradient on the screening properties of ionic fluids, Phys. Rev. Mater. 7 (4) (2023) 045803, http://dx.doi.org/10.1103/PhysRevMaterials.7.045803, arXiv:2212.12233. URL http://arxiv.org/abs/2212.12233https://link.aps.org/doi/10.1103/PhysRevMaterials.7.045803.

[154] M. Born, H. Green, A general kinetic theory of liquids I. The molecular distribution functions, Proc. R. Soc. Lond. Ser. A Math. Phys. Eng. Sci. 188 (1012) (1946) 10–18, http://dx.doi.org/10.1098/rspa.1946.0093, URL https://royalsocietypublishing.org/doi/10.1098/rspa.1946.0093.

[155] J. Yvon, La Théorie Statistique des Fluides et l'Équation d'État, Hermann, Paris, 1935.

[156] J.G. Kirkwood, Statistical mechanics of fluid mixtures, J. Chem. Phys. 3 (5) (1935) 300–313, http://dx.doi.org/10.1063/1.1749657, URL https://doi.org/10.1063/1.1749657https://pubs.aip.org/jcp/article/3/5/300/203696/Statistical-Mechanics-of-Fluid-Mixtures.

[157] N.N. Bogoliubov, Kinetic equations, J. Phys. USSR 10 (3) (1946) 265–274.

[158] M.V. Fedorov, A.A. Kornyshev, Ionic liquids at electrified interfaces, Chem. Rev. 114 (5) (2014) 2978–3036, http://dx.doi.org/10.1021/cr400374x.

[159] D.A. McQuarrie, Statistical Mechanics, in: G - Reference,Information and Interdisciplinary Subjects Series, University Science Books, 2000, pp. 254–289.

[160] J.-P. Hansen, I.R. McDonald, Theory of Simple Liquids : With Applications to Soft Matter, fourth ed., Elsevier Science & Technology, San Diego, United Kingdom, 2013, pp. 105–147, URL https://www.sciencedirect.com/book/9780123870322/theory-of-simple-liquids.

[161] J.P. de Souza, K. Pivnic, M.Z. Bazant, M. Urbakh, A.A. Kornyshev, Structural forces in ionic liquids: The role of ionic size asymmetry, J. Phys. Chem. B 126 (6) (2022) 1242–1253, http://dx.doi.org/10.1021/acs.jpcb.1c09441.

[162] R.M. Adar, T. Markovich, A. Levy, H. Orland, D. Andelman, Dielectric constant of ionic solutions: Combined effects of correlations and excluded volume, J. Chem. Phys. 149 (5) (2018) http://dx.doi.org/10.1063/1.5042235, arXiv:1806.01607.

[163] N. Gavish, K. Promislow, Dependence of the dielectric constant of electrolyte solutions on ionic concentration: A microfield approach, Phys. Rev. E 94 (1) (2016) 1–7, http://dx.doi.org/10.1103/PhysRevE.94.012611, arXiv:1208.5169.

[164] J.-P. Hansen, I.R. McDonald, Theory of Simple Liquids : With Applications to Soft Matter, fourth ed., Elsevier Science & Technology, San Diego, United Kingdom, 2013, pp. 408–416, URL https://www.sciencedirect.com/book/9780123870322/theory-of-simple-liquids.

[165] P. Cats, R. Evans, A. Härtel, R. Van Roij, Primitive model electrolytes in the near and far field: Decay lengths from DFT and simulations, J. Chem. Phys. 154 (12) (2021) http://dx.doi.org/10.1063/5.0039619, arXiv:2012.02713.

[166] J. Yang, S. Kondrat, C. Lian, H. Liu, A. Schlaich, C. Holm, Solvent effects on structure and screening in confined electrolytes, Phys. Rev. Lett. 131 (11) (2023) 118201, http://dx.doi.org/10.1103/PhysRevLett.131.118201, URL https://doi.org/10.1103/PhysRevLett.131.118201https://link.aps.org/doi/10.1103/PhysRevLett.131.118201.

[167] K. Ma, C. Lian, C.E. Woodward, B. Qin, Classical density functional theory reveals coexisting short-range structural decay and long-range force decay in ionic liquids, Chem. Phys. Lett. 739 (December 2019) (2020) http://dx.doi.org/10.1016/j.cplett.2019.137001.

[168] M. Bültmann, A. Härtel, The primitive model in classical density functional theory: beyond the standard mean-field approximation, J. Phys.: Condens. Matter 34 (23) (2022) 235101, http://dx.doi.org/10.1088/1361-648X/ac5e7a, URL https://iopscience.iop.org/article/10.1088/1361-648X/ac5e7a.

[169] P. Cats, R. van Roij, The differential capacitance as a probe for the electric double layer structure and the electrolyte bulk composition, J. Chem. Phys. 155 (10) (2021) http://dx.doi.org/10.1063/5.0064315, arXiv:2107.10514.

[170] P. Cats, A. Härtel, In-plane structure of the electric double layer in the primitive model using classical density functional theory, J. Chem. Phys. 159 (18) (2023) http://dx.doi.org/10.1063/5.0176309.

[171] J. Zeman, S. Kondrat, C. Holm, Ionic screening in bulk and under confinement, J. Chem. Phys. 155 (20) (2021) http://dx.doi.org/10.1063/5.0069340.

[172] R. Kjellander, Focus article: Oscillatory and long-range monotonic exponential decays of electrostatic interactions in ionic liquids and other electrolytes: The significance of dielectric permittivity and renormalized charges, J. Chem. Phys. 148 (19) (2018) http://dx.doi.org/10.1063/1.5010024.

[173] P. Keblinski, J. Eggebrecht, D. Wolf, S.R. Phillpot, Molecular dynamics study of screening in ionic fluids, J. Chem. Phys. 113 (1) (2000) 282–291, http://dx.doi.org/10.1063/1.481819.

[174] A.R. Finney, I.J. McPherson, P.R. Unwin, M. Salvalaglio, Electrochemistry, ion adsorption and dynamics in the double layer: A study of NaCl(aq) on graphite, Chem. Sci. 12 (33) (2021) 11166–11180, http://dx.doi.org/10.1039/d1sc02289j, arXiv:2104.11773.

[175] P. Jones, F. Coupette, A. Härtel, A.A. Lee, Bayesian unsupervised learning reveals hidden structure in concentrated electrolytes, J. Chem. Phys. 154 (13) (2021) http://dx.doi.org/10.1063/5.0039617, arXiv:2012.10694.

[176] F. Coupette, A.A. Lee, A. Härtel, Screening lengths in ionic fluids, Phys. Rev. Lett. 121 (7) (2018) 75501, http://dx.doi.org/10.1103/PhysRevLett.121.075501, arXiv:1803.10596.

[177] E. Krucker-Velasquez, J.W. Swan, Underscreening and hidden ion structures in large scale simulations of concentrated electrolytes, J. Chem. Phys. 155 (13) (2021) http://dx.doi.org/10.1063/5.0061230, arXiv:2106.13197. URL http://arxiv.org/abs/2106.13197.

[178] M.A. Gebbie, A.M. Smith, H.A. Dobbs, A.A. Lee, G.G. Warr, X. Banquy, M. Valtiner, M.W. Rutland, J.N. Israelachvili, S. Perkin, R. Atkin, Long range electrostatic forces in ionic liquids, Chem. Commun. 53 (7) (2017) 1214–1224, http://dx.doi.org/10.1039/c6cc08820a.

[179] M.A. Gebbie, H.A. Dobbs, M. Valtiner, J.N. Israelachvili, Long-range electrostatic screening in ionic liquids, Proc. Natl. Acad. Sci. USA 112 (24) (2015) 7432–7437, http://dx.doi.org/10.1073/pnas.1508366112.

[180] D.R. MacFarlane, M. Forsyth, E.I. Izgorodina, A.P. Abbott, G. Annat, K. Fraser, On the concept of ionicity in ionic liquids, Phys. Chem. Chem. Phys. 11 (25) (2009) 4962–4967, http://dx.doi.org/10.1039/b900201d.

[181] H. Tokuda, S. Tsuzuki, M.A.B.H. Susan, K. Hayamizu, M. Watanabe, How ionic are room-temperature ionic liquids? An indicator of the physicochemical properties, J. Phys. Chem. B 110 (39) (2006) 19593–19600, http://dx.doi.org/10.1021/jp064159v.

[182] S. Perkin, M. Salanne, P. Madden, R. Lynden-Bell, Is a stern and diffuse layer model appropriate to ionic liquids at surfaces? Proc. Natl. Acad. Sci. USA 110 (44) (2013) 4121, http://dx.doi.org/10.1073/pnas.1314188110.

[183] T.S. Groves, S. Perkin, Wave mechanics in an ionic liquid mixture, 2024, arXiv:/arxiv.org/html/2402.17480v1.

[184] A. Rohatgi, Webplotdigitizer: Version 4.6, 2022, URL https://automeris.io/WebPlotDigitizer.

[185] W. Lin, J. Klein, Direct measurement of surface forces: Recent advances and insights, Appl. Phys. Rev. 8 (3) (2021) 031316, http://dx.doi.org/10.1063/5.0059893.

[186] H. Hayler, T.S. Groves, A. Guerrini, A. Southam, W. Zheng, S. Perkin, The surface force balance: Direct measurement of interactions in fluids and soft matter, Rep. Progr. Phys. (2024) http://dx.doi.org/10.1088/1361-6633/ad2b9b, URL http://iopscience.iop.org/article/10.1088/1361-6633/ad2b9bhttps://iopscience.iop.org/article/10.1088/1361-6633/ad2b9b.

[187] C. Malmberg, A. Maryott, Dielectric constant of water from 0 to 100 C, J. Res. Natl. Bur. Stand. 56 (1) (1956) 1, http://dx.doi.org/10.6028/jres.056.001, URL https://nvlpubs.nist.gov/nistpubs/jres/56/jresv56n1p1_A1b.pdf.

[188] B.B. Owen, R.C. Miller, C.E. Milner, H.L. Cogan, The dielectric constant of water as a function of temperature and pressure 1,2, J. Phys. Chem. 65 (11) (1961) 2065–2070, http://dx.doi.org/10.1021/j100828a035, URL https://doi.org/10.1021/j100828a035https://pubs.acs.org/doi/abs/10.1021/j100828a035.

[189] M. Mizoshiri, T. Nagao, Y. Mizoguchi, M. Yao, Dielectric permittivity of room temperature ionic liquids: A relation to the polar and nonpolar domain structures, J. Chem. Phys. 132 (16) (2010) http://dx.doi.org/10.1063/1.3419906.

[190] J. Israelachvili, Intermolecular and Surface Forces, third ed., Elsevier, 2011, http://dx.doi.org/10.1016/C2009-0-21560-1, URL https://linkinghub.elsevier.com/retrieve/pii/C20090215601.

[191] R. Lhermerout, S. Perkin, Nanoconfined ionic liquids: Disentangling electrostatic and viscous forces, Phys. Rev. Fluids 3 (1) (2018) 1–13, http://dx.doi.org/10.1103/PhysRevFluids.3.014201, arXiv:1801.00955.

[192] H.W. Cheng, P. Stock, B. Moeremans, T. Baimpos, X. Banquy, F.U. Renner, M. Valtiner, Characterizing the influence of water on charging and layering at electrified ionic-liquid/solid interfaces, Adv. Mater. Interfaces 2 (12) (2015) 1–9, http://dx.doi.org/10.1002/admi.201500159.

[193] R.M. Espinosa-Marzal, A. Arcifa, A. Rossi, N.D. Spencer, Ionic liquids confined in hydrophilic nanocontacts: Structure and lubricity in the presence of water, J. Phys. Chem. C 118 (12) (2014) 6491–6503, http://dx.doi.org/10.1021/jp5000123.

[194] R. An, A. Laaksonen, M. Wu, Y. Zhu, F.U. Shah, X. Lu, X. Ji, Atomic force microscopy probing interactions and microstructures of ionic liquids at solid surfaces, Nanoscale (2022) 11098–11128, http://dx.doi.org/10.1039/d2nr02812c.

[195] M. Han, R.M. Espinosa-Marzal, Influence of water on structure, dynamics, and electrostatics of hydrophilic and hydrophobic ionic liquids in charged and hydrophilic confinement between mica surfaces, ACS Appl. Mater. Interfaces 11 (36) (2019) 33465–33477, http://dx.doi.org/10.1021/acsami.9b10923.

[196] C. Fung, R. Sedev, S. Miklavcic, J.N. Connor, Influence of electric field on the structure of a nanoconfined concentrated electrolyte, in: Chemeca 2016: Chemical Engineering - Regeneration, Recovery and Reinvention, Engineers Australia, Melbourne, Vic., 2016, pp. 391–399, http://dx.doi.org/10.3316/informit.406066786855549, 2016: 391-399. (September). URL https://search.informit.org/doi/10.3316/informit.406066786855549.

[197] R. Lhermerout, The influence of mechanical deformations on surface force measurements, Lubricants 9 (7) (2021) http://dx.doi.org/10.3390/lubricants9070069, arXiv:2001.01090.

[198] P. Gaddam, R. Grayson, W. Ducker, Adsorption at confined interfaces, Langmuir 34 (36) (2018) 10469–10479, http://dx.doi.org/10.1021/acs.langmuir.8b01418.

[199] A. Ciach, O. Patsahan, Correct scaling of the correlation length from a theory for concentrated electrolytes, J. Phys. Condens. Matter 33 (37) (2021) http://dx.doi.org/10.1088/1361-648X/ac0f9e, arXiv:2102.00878.

[200] A. Ciach, O. Patsahan, Structure of ionic liquids and concentrated electrolytes from a mesoscopic theory, J. Mol. Liq. 377 (2022) 121453, http://dx.doi.org/10.1016/j.molliq.2023.121453, arXiv:2211.02367. URL http://arxiv.org/abs/2211.02367.

[201] G.V. Franks, Zeta potentials and yield stresses of silica suspensions in concentrated monovalent electrolytes: Isoelectric point shift and additional attraction, J. Colloid Interface Sci. 249 (1) (2002) 44–51, http://dx.doi.org/10.1006/jcis.2002.8250, URL https://linkinghub.elsevier.com/retrieve/pii/S0021979702982500.

[202] S.B. Johnson, G.V. Franks, P.J. Scales, T.W. Healy, Binding of monovalent electrolyte ions on α-alumina. II. The shear yield stress of concentrated suspensions, Langmuir 15 (8) (1999) 2844–2853, http://dx.doi.org/10.1021/la9808768.

[203] D.F. Parsons, M. Boström, T.J. Maceina, A. Salis, B.W. Ninham, Why direct or reversed Hofmeister series? Interplay of hydration, non-electrostatic potentials, and ion size, Langmuir 26 (5) (2010) 3323–3328, http://dx.doi.org/10.1021/la903061h, URL https://pubs.acs.org/doi/10.1021/la903061h.

[204] N. Schwierz, D. Horinek, U. Sivan, R.R. Netz, Reversed Hofmeister series—The rule rather than the exception, 2016, http://dx.doi.org/10.1016/j.cocis.2016.04.003.

[205] N.R. Aluru, F. Aydin, M.Z. Bazant, D. Blankschtein, A.H. Brozena, J.P. de Souza, M. Elimelech, S. Faucher, J.T. Fourkas, V.B. Koman, M. Kuehne, H.J. Kulik, H.-K. Li, Y. Li, Z. Li, A. Majumdar, J. Martis, R.P. Misra, A. Noy, T.A. Pham, H. Qu, A. Rayabharam, M.A. Reed, C.L. Ritt, E. Schwegler, Z. Siwy, M.S. Strano, Y. Wang, Y.-C. Yao, C. Zhan, Z. Zhang, Fluids and electrolytes under confinement in single-digit nanopores, Chem. Rev. 123 (6) (2023) 2737–2831, http://dx.doi.org/10.1021/acs.chemrev.2c00155, URL https://pubs.acs.org/doi/10.1021/acs.chemrev.2c00155.

[206] D. Muñoz-Santiburcio, D. Marx, Confinement-controlled aqueous chemistry within nanometric slit pores, Chem. Rev. 121 (11) (2021) 6293–6320, http://dx.doi.org/10.1021/acs.chemrev.0c01292.

[207] S. Kondrat, G. Feng, F. Bresme, M. Urbakh, A.A. Kornyshev, Theory and simulations of ionic liquids in nanoconfinement, Chem. Rev. 123 (10) (2023) 6668–6715, http://dx.doi.org/10.1021/acs.chemrev.2c00728.

[208] D.L. Gurina, E.G. Odintsova, Y.A. Budkov, Disjoining pressure decay length in room-temperature ionic liquids: A molecular simulation study, J. Phys. Chem. B (2024) 10–13, http://dx.doi.org/10.1021/acs.jpcb.3c08425, URL https://pubs.acs.org/doi/10.1021/acs.jpcb.3c08425.

[209] B. Stojimirović, M. Galli, G. Trefalt, Forces between silica particles in isopropanol solutions of 1:1 electrolytes, Phys. Rev. Res. 2 (2) (2020) 023315, http://dx.doi.org/10.1103/PhysRevResearch.2.023315, arXiv:2003.04058. URL https://link.aps.org/doi/10.1103/PhysRevResearch.2.023315.

[210] N. Hjalmarsson, R. Atkin, M.W. Rutland, Switchable long-range double layer force observed in a protic ionic liquid, Chem. Commun. 53 (3) (2017) 647–650, http://dx.doi.org/10.1039/C6CC07396D.

[211] M. Radiom, P. Pedraz, G. Pilkington, P. Rohlmann, S. Glavatskih, M.W. Rutland, Anomalous interfacial structuring of a non-halogenated ionic liquid: Effect of substrate and temperature, Colloids Interfaces 2 (4) (2018) 1–14, http://dx.doi.org/10.3390/colloids2040060.

[212] F. Grün, M. Jardat, P. Turq, C. Amatore, Relaxation of the electrical double layer after an electron transfer approached by Brownian dynamics simulation, J. Chem. Phys. 120 (20) (2004) 9648–9655, http://dx.doi.org/10.1063/1.1718201.

[213] M. Belotti, X. Lyu, L. Xu, P. Halat, N. Darwish, D.S. Silvester, C. Goh, E.I. Izgorodina, M.L. Coote, S. Ciampi, Experimental evidence of long-lived electric fields of ionic liquid bilayers, J. Am. Chem. Soc. 143 (42) (2021) 17431–17440, http://dx.doi.org/10.1021/jacs.1c06385.

[214] A.G. Moreira, R.R. Netz, Binding of similarly charged plates with counterions only, Phys. Rev. Lett. 87 (7) (2001) 78301–1–78301–4, http://dx.doi.org/10.1103/PhysRevLett.87.078301.

[215] S.S. Lee, A. Koishi, I.C. Bourg, P. Fenter, Ion correlations drive charge overscreening and heterogeneous nucleation at solid-aqueous electrolyte interfaces, Proc. Natl. Acad. Sci. USA 118 (32) (2021) 1–7, http://dx.doi.org/10.1073/pnas.2105154118.

[216] J. Neumann, S.S. Lee, E.J. Zhao, P. Fenter, Direct experimental observations of ion distributions during overcharging at the muscovite-water interface by adsorption of Rb+ and halides (Cl-, Br-, I-) at high salinity, ChemPhysChem 202300545 (2023) 28–30, http://dx.doi.org/10.1002/cphc.202300545.

[217] R. Funari, A. Matsumoto, J.R. De Bruyn, A.Q. Shen, Rheology of the electric double layer in electrolyte solutions, Anal. Chem. 92 (12) (2020) 8244–8253, http://dx.doi.org/10.1021/acs.analchem.0c00475.

[218] G. Franceschi, P. Kocán, A. Conti, S. Brandstetter, J. Balajka, I. Sokolović, M. Valtiner, F. Mittendorfer, M. Schmid, M. Setvín, U. Diebold, Resolving the intrinsic short-range ordering of K+ ions on cleaved muscovite mica, Nature Commun. 14 (1) (2023) 1–8, http://dx.doi.org/10.1038/s41467-023-35872-y.

[219] L.T. Zhuravlev, The surface chemistry of amorphous silica. Zhuravlev model, Colloids Surf. A 173 (1–3) (2000) 1–38, http://dx.doi.org/10.1016/S0927-7757(00)00556-2.

[220] A.M. Schrader, J.I. Monroe, R. Sheil, H.A. Dobbs, T.J. Keller, Y. Li, S. Jain, M.S. Shell, J.N. Israelachvili, S. Han, Surface chemical heterogeneity modulates silica surface hydration, Proc. Natl. Acad. Sci. USA 115 (12) (2018) 2890–2895, http://dx.doi.org/10.1073/pnas.1722263115.

[221] C. Macias-Romero, I. Nahalka, H.I. Okur, S. Roke, Optical imaging of surface chemistry and dynamics in confinement, Science 357 (6353) (2017) 784–788, http://dx.doi.org/10.1126/science.aal4346, URL https://www.science.org/doi/10.1126/science.aal4346.

[222] M. Kosmulski, The pH dependent surface charging and points of zero charge. X. Update, Adv. Colloid Interface Sci. 319 (July) (2023) 102973, http://dx.doi.org/10.1016/j.cis.2023.102973, URL https://doi.org/10.1016/j.cis.2023.102973https://linkinghub.elsevier.com/retrieve/pii/S0001868623001409.

[223] D. Wang, Y. Tian, L. Jiang, Abnormal properties of low-dimensional confined water, Small 17 (31) (2021) http://dx.doi.org/10.1002/smll.202100788.

[224] S. Gekle, R.R. Netz, Anisotropy in the dielectric spectrum of hydration water and its relation to water dynamics, J. Chem. Phys. 137 (10) (2012) http://dx.doi.org/10.1063/1.4749380, URL https://pubs.aip.org/jcp/article/137/10/104704/191937/Anisotropy-in-the-dielectric-spectrum-of-hydration.

[225] L. Fumagalli, A. Esfandiar, R. Fabregas, S. Hu, P. Ares, A. Janardanan, Q. Yang, B. Radha, T. Taniguchi, K. Watanabe, G. Gomila, K.S. Novoselov, A.K. Geim, Anomalously low dielectric constant of confined water, Science 360 (6395) (2018) 1339–1342, http://dx.doi.org/10.1126/science.aat4191.

[226] P. Loche, L. Scalfi, M. Ali Amu, O. Schullian, D.J. Bonthuis, B. Rotenberg, R.R. Netz, Effects of surface rigidity and metallicity on dielectric properties and ion interactions at aqueous hydrophobic interfaces, J. Chem. Phys. 157 (9) (2022) http://dx.doi.org/10.1063/5.0101509.

[227] J.-F. Olivieri, J.T. Hynes, D. Laage, Confined water's dielectric constant reduction is due to the surrounding low dielectric media and not to interfacial molecular ordering, J. Phys. Chem. Lett. 12 (17) (2021) 4319–4326, http://dx.doi.org/10.1021/acs.jpclett.1c00447, URL https://pubs.acs.org/doi/10.1021/acs.jpclett.1c00447.

[228] H. Zhu, A. Ghoufi, A. Szymczyk, B. Balannec, D. Morineau, Anomalous dielectric behavior of nanoconfined electrolytic solutions, Phys. Rev. Lett. 109 (10) (2012) 1–5, http://dx.doi.org/10.1103/PhysRevLett.109.107801.

[229] H. Zhu, A. Ghoufi, A. Szymczyk, B. Balannec, D. Morineau, Zhu et al. Reply, Phys. Rev. Lett. 111 (8) (2013) 1–2, http://dx.doi.org/10.1103/PhysRevLett.111.089802.

[230] H. Jalali, E. Lotfi, R. Boya, M. Neek-Amal, Abnormal dielectric constant of nanoconfined water between graphene layers in the presence of salt, J. Phys. Chem. B 125 (6) (2021) 1604–1610, http://dx.doi.org/10.1021/acs.jpcb.0c09156.

[231] T.R. Underwood, I.C. Bourg, Dielectric properties of water in charged nanopores, J. Phys. Chem. B 126 (14) (2022) 2688–2698, http://dx.doi.org/10.1021/acs.jpcb.1c09688.

[232] P. Loche, C. Ayaz, A. Schlaich, D.J. Bonthuis, R.R. Netz, Breakdown of linear dielectric theory for the interaction between hydrated ions and graphene, J. Phys. Chem. Lett. 9 (22) (2018) 6463–6468, http://dx.doi.org/10.1021/acs.jpclett.8b02473.

[233] P. Loche, C. Ayaz, A. Wolde-Kidan, A. Schlaich, R.R. Netz, Universal and nonuniversal aspects of electrostatics in aqueous nanoconfinement, J. Phys. Chem. B 124 (21) (2020) 4365–4371, http://dx.doi.org/10.1021/acs.jpcb.0c01967.

[234] E. Papadopoulou, J. Zavadlav, R. Podgornik, M. Praprotnik, P. Koumoutsakos, Tuning the dielectric response of water in nanoconfinement through surface wettability, ACS Nano 15 (12) (2021) 20311–20318, http://dx.doi.org/10.1021/acsnano.1c08512.

[235] M.H. Motevaselian, N.R. Aluru, Universal reduction in dielectric response of confined fluids, ACS Nano 14 (10) (2020) 12761–12770, http://dx.doi.org/10.1021/acsnano.0c03173, URL https://pubs.acs.org/doi/10.1021/acsnano.0c03173.

[236] D.V. Matyushov, Dielectric susceptibility of water in the interface, J. Phys. Chem. B 125 (30) (2021) 8282–8293, http://dx.doi.org/10.1021/acs.jpcb.1c03720.

[237] G. Monet, H. Berthoumieux, F. Bresme, A. Kornyshev, Nonlocal dielectric response of water in nanoconfinement, Phys. Rev. Lett. 126 (21) (2021) 216001, http://dx.doi.org/10.1103/PhysRevLett.126.216001, arXiv:2102.09309.

[238] A. Ciach, O. Patsahan, Mesoscopic theory for ionic liquids and concentrated electrolytes in a slit with charged walls, J. Mol. Liq. 382 (April) (2023) 121949, http://dx.doi.org/10.1016/j.molliq.2023.121949, URL https://doi.org/10.1016/j.molliq.2023.121949https://linkinghub.elsevier.com/retrieve/pii/S0167732223007523.

[239] J. Huang, Confinement induced dilution: Electrostatic screening length anomaly in concentrated electrolytes in confined space, J. Phys. Chem. C 122 (6) (2018) 3428–3433, http://dx.doi.org/10.1021/acs.jpcc.7b11093.

[240] Z.X. Luo, Y.Z. Xing, Y.C. Ling, A. Kleinhammes, Y. Wu, Electroneutrality breakdown and specific ion effects in nanoconfined aqueous electrolytes observed by NMR, Nature Commun. 6 (2015) http://dx.doi.org/10.1038/ncomms7358.

[241] T. Colla, M. Girotto, A.P. Dos Santos, Y. Levin, Charge neutrality breakdown in confined aqueous electrolytes: Theory and simulation, J. Chem. Phys. 145 (9) (2016) http://dx.doi.org/10.1063/1.4962198, arXiv:1609.00619.

[242] S.A. Safran, P. Pincus, Scaling perspectives of underscreening in concentrated electrolyte solutions, Soft Matter 1 (2023) 1–285, http://dx.doi.org/10.1039/D3SM01094E, URL http://pubs.rsc.org/en/Content/ArticleLanding/2023/SM/D3SM01094E.

[243] Y. Marcus, G. Hefter, Ion pairing, Chem. Rev. 106 (11) (2006) 4585–4621, http://dx.doi.org/10.1021/cr040087x.

[244] N.F. Van Der Vegt, K. Haldrup, S. Roke, J. Zheng, M. Lund, H.J. Bakker, Water-mediated ion pairing: Occurrence and relevance, Chem. Rev. 116 (13) (2016) 7626–7641, http://dx.doi.org/10.1021/acs.chemrev.5b00742.

[245] Y. Marcus, Effect of ions on the structure of water: Structure making and breaking, Chem. Rev. 109 (3) (2009) 1346–1370, http://dx.doi.org/10.1021/cr8003828.

[246] G. Schwaab, F. Sebastiani, M. Havenith, Ion hydration and ion pairing as probed by THz spectroscopy, Angew. Chem. Int. Edn 58 (10) (2019) 3000–3013, http://dx.doi.org/10.1002/anie.201805261.

[247] Y. Marcus, Ions in solution and their solvation, 2015, pp. 1–293, http://dx.doi.org/10.1002/9781118892336.

[248] H.J. Bakker, Structural dynamics of aqueous salt solutions, Chem. Rev. 108 (4) (2008) 1456–1473, http://dx.doi.org/10.1021/cr0206622.

[249] H. Ohtaki, T. Radnai, Structure and dynamics of hydrated ions, Chem. Rev. 93 (3) (1993) 1157–1204, http://dx.doi.org/10.1021/cr00019a014.

[250] G.R. Elliott, E. Wanless, G.B. Webber, G.G. Andersson, V.S.J. Craig, A. Page, Dynamic ion-ion correlations and ion-pair lifetimes in aqueous electrolytes, J. Phys. Chem. B (2023) submitted for publication.

[251] R.M. Adar, T. Markovich, D. Andelman, Bjerrum pairs in ionic solutions: A Poisson-Boltzmann approach, J. Chem. Phys. 146 (19) (2017) http://dx.doi.org/10.1063/1.4982885, arXiv:1702.04853.

[252] R. Buchner, T. Chen, G. Hefter, Complexity in “simple” electrolyte solutions: Ion pairing in MgSO4(aq), J. Phys. Chem. B 108 (7) (2004) 2365–2375, http://dx.doi.org/10.1021/jp034870p.

[253] W. Wachter, Š. Fernandez, R. Buchner, G. Hefter, Ion association and hydration in aqueous solutions of LiCl and Li 2 SO 4 by dielectric spectroscopy, J. Phys. Chem. B 111 (30) (2007) 9010–9017, http://dx.doi.org/10.1021/jp072425e, URL https://pubs.acs.org/doi/10.1021/jp072425e.

[254] R. Buchner, G. Hefter, Ion hydration and association in aqueous solutions of zinc sulfate by dielectric spectroscopy, J. Mol. Liq. 383 (March) (2023) 122146, http://dx.doi.org/10.1016/j.molliq.2023.122146.

[255] R. Kjellander, Statistical Mechanics of Liquids and Solutions, CRC Press, 2019, pp. 285–286, http://dx.doi.org/10.1201/9780429194368.

[256] Y. Zhang, E.J. Maginn, Direct correlation between ionic liquid transport properties and ion pair lifetimes: A molecular dynamics study, J. Phys. Chem. Lett. 6 (4) (2015) 700–705, http://dx.doi.org/10.1021/acs.jpclett.5b00003.

[257] J.G. McDaniel, C.Y. Son, Ion correlation and collective dynamics in BMIM/BF4-based organic electrolytes: From dilute solutions to the ionic liquid limit, J. Phys. Chem. B 122 (28) (2018) 7154–7169, http://dx.doi.org/10.1021/acs.jpcb.8b04886.

[258] D.F. Parsons, M. Boström, P.L. Nostro, B.W. Ninham, Hofmeister effects: Interplay of hydration, nonelectrostatic potentials, and ion size, 2011, http://dx.doi.org/10.1039/c1cp20538b.

[259] T. Hoang Ngoc Minh, B. Rotenberg, S. Marbach, Ionic fluctuations in finite volumes: fractional noise and hyperuniformity, Faraday Discuss. (2023) http://dx.doi.org/10.1039/d3fd00031a, arXiv:2302.03393.

[260] S. Torquato, Hyperuniform states of matter, Phys. Rep. 745 (2018) 1–95, http://dx.doi.org/10.1016/j.physrep.2018.03.001, arXiv:1801.06924.

[261] B. Sellner, M. Valiev, S.M. Kathmann, Charge and electric field fluctuations in aqueous NaCl electrolytes, J. Phys. Chem. B 117 (37) (2013) 10869–10882, http://dx.doi.org/10.1021/jp405578w.

[262] E.O. Fetisov, C.J. Mundy, G.K. Schenter, C.J. Benmore, J.L. Fulton, S.M. Kathmann, Nanometer-scale correlations in aqueous salt solutions, J. Phys. Chem. Lett. 11 (7) (2020) 2598–2604, http://dx.doi.org/10.1021/acs.jpclett.0c00322.

[263] M. Apostol, Screening length in concentrated electrolytes, Chem. Phys. 558 (January) (2022) 111514, http://dx.doi.org/10.1016/j.chemphys.2022.111514.

[264] W.A. Jacak, Plasmons in finite spherical electrolyte systems: RPA effective jellium model for ionic plasma excitations, Plasmonics 11 (2) (2016) 637–651, http://dx.doi.org/10.1007/s11468-015-0064-6.

[265] C. David, Two-fluid, hydrodynamic model for spherical electrolyte systems, Sci. Rep. 8 (1) (2018) 7544, http://dx.doi.org/10.1038/s41598-018-25791-0, URL http://www.nature.com/articles/s41598-018-25791-0.

[266] T.E. Markland, M. Ceriotti, Nuclear quantum effects enter the mainstream, Nat. Rev. Chem. 2 (3) (2018) http://dx.doi.org/10.1038/s41570-017-0109, arXiv:1803.01037.

[267] M. Ceriotti, W. Fang, P.G. Kusalik, R.H. McKenzie, A. Michaelides, M.A. Morales, T.E. Markland, Nuclear quantum effects in water and aqueous systems: Experiment, theory, and current challenges, Chem. Rev. 116 (13) (2016) 7529–7550, http://dx.doi.org/10.1021/acs.chemrev.5b00674.

[268] C. Schran, O. Marsalek, T.E. Markland, Unravelling the influence of quantum proton delocalization on electronic charge transfer through the hydrogen bond, Chem. Phys. Lett. 678 (2017) 289–295, http://dx.doi.org/10.1016/j.cplett.2017.04.034, arXiv:1703.06243.

[269] B.R. Shrestha, S. Pillai, A. Santana, S.H. Donaldson, T.A. Pascal, H. Mishra, Nuclear quantum effects in hydrophobic nanoconfinement, J. Phys. Chem. Lett. 10 (18) (2019) 5530–5535, http://dx.doi.org/10.1021/acs.jpclett.9b01835.

[270] A.K. Soper, C.J. Benmore, Quantum differences between heavy and light water, Phys. Rev. Lett. 101 (6) (2008) 1–4, http://dx.doi.org/10.1103/PhysRevLett.101.065502.

[271] J. Xu, Z. Sun, C. Zhang, M. Dellostritto, D. Lu, M.L. Klein, X. Wu, Importance of nuclear quantum effects on the hydration of chloride ion, Phys. Rev. Mater. 5 (1) (2021) L012801, http://dx.doi.org/10.1103/PhysRevMaterials.5.L012801, arXiv:2009.07304.

[272] J.D. Mallory, V.A. Mandelshtam, Nuclear quantum effects and thermodynamic properties for small (H2O)1-21X- Clusters (X-=F-, Cl-, Br-, I-), J. Phys. Chem. A 122 (16) (2018) 4167–4180, http://dx.doi.org/10.1021/acs.jpca.8b00917.

[273] E.C. Noonan, Solubility of salts in deuterium oxide, J. Am. Chem. Soc. 70 (9) (1948) 2915–2918, http://dx.doi.org/10.1021/ja01189a026, URL https://doi.org/10.1021/ja01189a026https://pubs.acs.org/doi/abs/10.1021/ja01189a026.

[274] O. Bonner, The osmotic and activity coefficients of some solutes in deuterium oxide, J. Chem. Thermodyn. 3 (6) (1971) 837–841, http://dx.doi.org/10.1016/S0021-9614(71)80012-5, URL https://www.sciencedirect.com/science/article/pii/S0021961471800125.

[275] N. Dupertuis, O.B. Tarun, C. Lütgebaucks, S. Roke, Three-dimensional confinement of water: H2O exhibits long-range (>50 nm) structure while D2O does not, Nano Lett. 22 (18) (2022) 7394–7400, http://dx.doi.org/10.1021/acs.nanolett.2c02206, URL https://pubs.acs.org/doi/10.1021/acs.nanolett.2c02206.

[276] R.C. Remsing, Modeling nuclear quantum effects on long-range electrostatics in nonuniform fluids, J. Chem. Phys. 159 (23) (2023) 234101, http://dx.doi.org/10.1063/5.0175808, URL https://doi.org/10.1063/5.0175808https://pubs.aip.org/jcp/article/159/23/234101/2929719/Modeling-nuclear-quantum-effects-on-long-range.

[277] P. Jia, J. Zhao, Single chain contraction and re-expansion of polystyrene sulfonate: A study on its re-entrant condensation at single molecular level, J. Chem. Phys. 131 (23) (2009) http://dx.doi.org/10.1063/1.3276278.

[278] D.F. Parsons, B.W. Ninham, Surface charge reversal and hydration forces explained by ionic dispersion forces and surface hydration, Colloids Surf. A 383 (1–3) (2011) 2–9, http://dx.doi.org/10.1016/j.colsurfa.2010.12.025.

[279] R.M. Pashley, J.N. Israelachvili, Dlvo and hydration forces between mica surfaces in Mg2+, Ca2+, Sr2+, and Ba2+ chloride solutions, J. Colloid Interface Sci. 97 (2) (1984) 446–455, http://dx.doi.org/10.1016/0021-9797(84)90316-3.

[280] E.I. Izgorodina, D. Golze, R. Maganti, V. Armel, M. Taige, T.J. Schubert, D.R. Macfarlane, Importance of dispersion forces for prediction of thermodynamic and transport properties of some common ionic liquids, Phys. Chem. Chem. Phys. 16 (16) (2014) 7209–7221, http://dx.doi.org/10.1039/c3cp53035c.

[281] D.K. Pandey, A. Materny, J. Kiefer, D.K. Singh, Quantification of the interactions in halide-anion-based imidazolium ionic liquids, J. Ion. Liquids 2 (2) (2022) 100032, http://dx.doi.org/10.1016/j.jil.2022.100032.

[282] K. Low, S.Y. Tan, E.I. Izgorodina, An ab initio study of the structure and energetics of hydrogen bonding in ionic liquids, Front. Chem. 7 (APR) (2019) 1–16, http://dx.doi.org/10.3389/fchem.2019.00208.

[283] E.I. Izgorodina, Z.L. Seeger, D.L. Scarborough, S.Y. Tan, Quantum chemical methods for the prediction of energetic, physical, and spectroscopic properties of ionic liquids, Chem. Rev. 117 (10) (2017) 6696–6754, http://dx.doi.org/10.1021/acs.chemrev.6b00528.

[284] C. Møller, M.S. Plesset, Note on an approximation treatment for many-electron systems, Phys. Rev. 46 (7) (1934) 618–622, http://dx.doi.org/10.1103/PhysRev.46.618, URL https://link.aps.org/doi/10.1103/PhysRev.46.618.

[285] J. Hermann, R.A. DiStasio, A. Tkatchenko, First-principles models for van der waals interactions in molecules and materials: Concepts, theory, and applications, Chem. Rev. 117 (6) (2017) 4714–4758, http://dx.doi.org/10.1021/acs.chemrev.6b00446.

[286] D.G. Fedorov, T. Nagata, K. Kitaura, Exploring chemistry with the fragment molecular orbital method, Phys. Chem. Chem. Phys. 14 (21) (2012) 7562–7577, http://dx.doi.org/10.1039/C2CP23784A.

[287] J.L. Galvez Vallejo, C. Snowdon, R. Stocks, F. Kazemian, F.C. Yan Yu, C. Seidl, Z. Seeger, M. Alkan, D. Poole, B.M. Westheimer, M. Basha, M. De La Pierre, A. Rendell, E.I. Izgorodina, M.S. Gordon, G.M. Barca, Toward an extreme-scale electronic structure system, J. Chem. Phys. 159 (4) (2023) http://dx.doi.org/10.1063/5.0156399.

[288] T.T. Duignan, S.M. Kathmann, G.K. Schenter, C.J. Mundy, Toward a first-principles framework for predicting collective properties of electrolytes, Acc. Chem. Res. 54 (13) (2021) 2833–2843, http://dx.doi.org/10.1021/acs.accounts.1c00107.

[289] T.T. Duignan, G.K. Schenter, J.L. Fulton, T. Huthwelker, M. Balasubramanian, M. Galib, M.D. Baer, J. Wilhelm, J. Hutter, M. Del Ben, X.S. Zhao, C.J. Mundy, Quantifying the hydration structure of sodium and potassium ions: Taking additional steps on Jacob's ladder, Phys. Chem. Chem. Phys. 22 (19) (2020) 10641–10652, http://dx.doi.org/10.1039/c9cp06161d.

[290] N.R. Agrawal, R. Wang, Electrostatic correlation induced ion condensation and charge inversion in multivalent electrolytes, J. Chem. Theory Comput. 18 (10) (2022) 6271–6280, http://dx.doi.org/10.1021/acs.jctc.2c00607, arXiv:2205.14222.

[291] N.R. Agrawal, R. Kaur, C. Carraro, R. Wang, Ion correlation-driven like-charge attraction in multivalent salt solutions, J. Chem. Phys. 159 (24) (2023) http://dx.doi.org/10.1063/5.0181061.

[292] R.P. Misra, J.P. De Souza, D. Blankschtein, M.Z. Bazant, Theory of surface forces in multivalent electrolytes, Langmuir 35 (35) (2019) 11550–11565, http://dx.doi.org/10.1021/acs.langmuir.9b01110.

[293] C.S. Perez-Martinez, S. Perkin, Interfacial structure and boundary lubrication of a dicationic ionic liquid, Langmuir 35 (48) (2019) 15444–15450, http://dx.doi.org/10.1021/acs.langmuir.9b01415, arXiv:1907.11295. URL https://pubs.acs.org/doi/10.1021/acs.langmuir.9b01415.

[294] R. Downing, G.V. Bossa, S. May, The role of ion-ion correlations for the differential capacitance of ionic liquids, J. Phys. Chem. C 122 (50) (2018) 28537–28544, http://dx.doi.org/10.1021/acs.jpcc.8b09756.

[295] M. Jitvisate, J.R. Seddon, Direct measurement of the differential capacitance of solvent-free and dilute ionic liquids, J. Phys. Chem. Lett. 9 (1) (2018) 126–131, http://dx.doi.org/10.1021/acs.jpclett.7b02946.

[296] A.A. Kornyshev, Double-layer in ionic liquids: Paradigm change? J. Phys. Chem. B 111 (20) (2007) 5545–5557, http://dx.doi.org/10.1021/jp067857o.

[297] T.Q. Nguyen, C. Breitkopf, Determination of diffusion coefficients using impedance spectroscopy data, J. Electrochem. Soc. 165 (14) (2018) E826–E831, http://dx.doi.org/10.1149/2.1151814jes.

[298] M.V. Khazimullin, Y.A. Lebedev, Influence of dielectric layers on estimates of diffusion coefficients and concentrations of ions from impedance spectroscopy, Phys. Rev. E 100 (6) (2019) 1–15, http://dx.doi.org/10.1103/PhysRevE.100.062601.

[299] M.O. de la Cruz, L. Belloni, M. Delsanti, J.P. Dalbiez, O. Spalla, M. Drifford, Precipitation of highly charged polyelectrolyte solutions in the presence of multivalent salts, J. Chem. Phys. 103 (13) (1995) 5781–5791, http://dx.doi.org/10.1063/1.470459.

[300] L. Valencia, E.M. Nomena, S. Monti, W. Rosas-Arbelaez, A.P. Mathew, S. Kumar, K.P. Velikov, Multivalent ion-induced re-entrant transition of carboxylated cellulose nanofibrils and its influence on nanomaterials' properties, Nanoscale 12 (29) (2020) 15652–15662, http://dx.doi.org/10.1039/d0nr02888f.

[301] F. Waggett, M.D. Shafiq, P. Bartlett, Failure of Debye–Hückel screening in low-charge colloidal suspensions, Colloids Interfaces 2 (4) (2018) 1–9, http://dx.doi.org/10.3390/colloids2040051.

[302] S. Kumar, I. Yadav, D. Ray, S. Abbas, D. Saha, V.K. Aswal, J. Kohlbrecher, Evolution of interactions in the protein solution as induced by mono and multivalent ions, Biomacromolecules 20 (5) (2019) 2123–2134, http://dx.doi.org/10.1021/acs.biomac.9b00374.

[303] W.S. Loo, X. Jiang, J.A. Maslyn, H.J. Oh, C. Zhu, K.H. Downing, N.P. Balsara, Reentrant phase behavior and coexistence in asymmetric block copolymer electrolytes, Soft Matter 14 (15) (2018) 2789–2795, http://dx.doi.org/10.1039/c8sm00175h.

[304] T. Wang, Y. Long, L. Liu, X. Wang, V.S. Craig, G. Zhang, G. Liu, Cation-specific conformational behavior of polyelectrolyte brushes: From aqueous to nonaqueous solvent, Langmuir 30 (43) (2014) 12850–12859, http://dx.doi.org/10.1021/la5033493.

[305] Y. Roiter, O. Trotsenko, V. Tokarev, S. Minko, Single molecule experiments visualizing adsorbed polyelectrolyte molecules in the full range of mono- and divalent counterion concentrations, J. Am. Chem. Soc. 132 (39) (2010) 13660–13662, http://dx.doi.org/10.1021/ja106065g.

[306] M. Hansch, B. Hämisch, R. Schweins, S. Prévost, K. Huber, Liquid-liquid phase separation in dilute solutions of poly(styrene sulfonate) with multivalent cations: Phase diagrams, chain morphology, and impact of temperature, J. Chem. Phys. 148 (1) (2018) http://dx.doi.org/10.1063/1.5006618.

[307] M. Biesalski, D. Johannsmann, J. Rühe, Electrolyte-induced collapse of a polyelectrolyte brush, J. Chem. Phys. 120 (18) (2004) 8807–8814, http://dx.doi.org/10.1063/1.1690242.

[308] Y. Tamura, A. Yoshimori, A. Suematsu, R. Akiyama, Reentrant crystallization of like-charged colloidal particles in an electrolyte solution: Relationship between the shape of the phase diagram and the effective potential of colloidal particles, Europhys. Lett. 129 (6) (2020) http://dx.doi.org/10.1209/0295-5075/129/66001.

[309] C.E. Sing, J.W. Zwanikken, M. Olvera De La Cruz, Effect of ion-ion correlations on polyelectrolyte gel collapse and reentrant swelling, Macromolecules 46 (12) (2013) 5053–5065, http://dx.doi.org/10.1021/ma400372p.

[310] M. Queralt-Martin, J.J. Perez-Grau, L.M. Alvero-Gonzalez, D.A. Perini, J. Cervera, V.M. Aguilella, A. Alcaraz, Biphasic concentration patterns in ionic transport under nanoconfinement revealed in steady state and time-dependent properties , J. Chem. Phys. 064701 (2023) http://dx.doi.org/10.1063/5.0136668.

[311] M. Han, R.M. Espinosa-Marzal, Strong stretching of poly(ethylene glycol) brushes mediated by ionic liquid solvation, J. Phys. Chem. Lett. 8 (17) (2017) 3954–3960, http://dx.doi.org/10.1021/acs.jpclett.7b01451.

[312] V. Kamysbayev, V. Srivastava, N.B. Ludwig, O.J. Borkiewicz, H. Zhang, J. Ilavsky, B. Lee, K.W. Chapman, S. Vaikuntanathan, D.V. Talapin, Nanocrystals in molten salts and ionic liquids: Experimental observation of ionic correlations extending beyond the debye length, ACS Nano 13 (5) (2019) 5760–5770, http://dx.doi.org/10.1021/acsnano.9b01292.

[313] G. Liu, D. Parsons, V.S.J. Craig, Re-entrant swelling and redissolution of polyelectrolytes arises from an increased electrostatic decay length at high salt concentrations, J. Colloid Interface Sci. 579 (2020) 369–378, http://dx.doi.org/10.1016/j.jcis.2020.06.072.

[314] Y. Li, M. Girard, M. Shen, J.A. Millan, M.O. De La Cruz, Strong attractions and repulsions mediated by monovalent salts, Proc. Natl. Acad. Sci. USA 114 (45) (2017) 11838–11843, http://dx.doi.org/10.1073/pnas.1713168114.

[315] C. Chang, V.L. Deringer, K.S. Katti, V. Van Speybroeck, C.M. Wolverton, Simulations in the era of exascale computing, Nat. Rev. Mater. 8 (May) (2023) 309–313, http://dx.doi.org/10.1038/s41578-023-00540-6.

[316] V. Gavini, S. Baroni, V. Blum, D.R. Bowler, A. Buccheri, J.R. Chelikowsky, S. Das, W. Dawson, P. Delugas, M. Dogan, C. Draxl, G. Galli, L. Genovese, P. Giannozzi, M. Giantomassi, X. Gonze, M. Govoni, F. Gygi, A. Gulans, J.M. Herbert, S. Kokott, T.D. Kühne, K.-H. Liou, T. Miyazaki, P. Motamarri, A. Nakata, J.E. Pask, C. Plessl, L.E. Ratcliff, R.M. Richard, M. Rossi, R. Schade, M. Scheffler, O. Schütt, P. Suryanarayana, M. Torrent, L. Truflandier, T.L. Windus, Q. Xu, V.W.-Z. Yu, D. Perez, Roadmap on electronic structure codes in the exascale era, Modelling Simul. Mater. Sci. Eng. 31 (6) (2023) 063301, http://dx.doi.org/10.1088/1361-651X/acdf06, URL https://iopscience.iop.org/article/10.1088/1361-651X/acdf06.

[317] J.A. Lemkul, J. Huang, B. Roux, A.D. Mackerell, An empirical polarizable force field based on the classical drude oscillator model: Development history and recent applications, Chem. Rev. 116 (9) (2016) 4983–5013, http://dx.doi.org/10.1021/acs.chemrev.5b00505.

[318] D. Bedrov, J.P. Piquemal, O. Borodin, A.D. MacKerell, B. Roux, C. Schröder, Molecular dynamics simulations of ionic liquids and electrolytes using polarizable force fields, Chem. Rev. 119 (13) (2019) 7940–7995, http://dx.doi.org/10.1021/acs.chemrev.8b00763.

[319] S. Garashchuk, V.A. Rassolov, Molecular dynamics with nuclear quantum effects: Approximations to the quantum force, 2020, pp. 41–90, http://dx.doi.org/10.1016/bs.arcc.2020.07.004, URL https://linkinghub.elsevier.com/retrieve/pii/S1574140020300049.

[320] T. Plé, N. Mauger, O. Adjoua, T.J. Inizan, L. Lagardère, S. Huppert, J.P. Piquemal, Routine molecular dynamics simulations including nuclear quantum effects: From force fields to machine learning potentials, J. Chem. Theory Comput. 19 (5) (2023) 1432–1445, http://dx.doi.org/10.1021/acs.jctc.2c01233, arXiv:2212.03137.

[321] M. Favaro, B. Jeong, P.N. Ross, J. Yano, Z. Hussain, Z. Liu, E.J. Crumlin, Unravelling the electrochemical double layer by direct probing of the solid/liquid interface, Nature Commun. 7 (May) (2016) 1–8, http://dx.doi.org/10.1038/ncomms12695.

[322] L. Van Hove, Correlations in space and time and born approximation scattering in systems of interacting particles, Phys. Rev. 95 (1) (1954) 249–262, http://dx.doi.org/10.1103/PhysRev.95.249.

[323] T. Iwashita, B. Wu, W.R. Chen, S. Tsutsui, A.Q. Baron, T. Egami, Seeing real-space dynamics of liquid water through inelastic x-ray scattering, Sci. Adv. 3 (12) (2017) 1–7, http://dx.doi.org/10.1126/sciadv.1603079.

[324] Y. Shinohara, W. Dmowski, T. Iwashita, B. Wu, D. Ishikawa, A.Q. Baron, T. Egami, Viscosity and real-space molecular motion of water: Observation with inelastic x-ray scattering, Phys. Rev. E 98 (2) (2018) 1–9, http://dx.doi.org/10.1103/PhysRevE.98.022604.

[325] R.A. Matsumoto, M.W. Thompson, V.Q. Vuong, W. Zhang, Y. Shinohara, A.C. Van Duin, P.R. Kent, S. Irle, T. Egami, P.T. Cummings, Investigating the accuracy of water models through the van hove correlation function, J. Chem. Theory Comput. 17 (10) (2021) 5992–6005, http://dx.doi.org/10.1021/acs.jctc.1c00637.

[326] R. Buchner, What can be learnt from dielectric relaxation spectroscopy about ion solvation and association? Pure Appl. Chem. 80 (6) (2008) 1239–1252, http://dx.doi.org/10.1351/pac200880061239.

[327] J. Barthel, R. Buchner, P.N. Eberspächer, M. Münsterer, J. Stauber, B. Wurm, Dielectric relaxation spectroscopy of electrolyte solutions. Recent developments and prospects, J. Mol. Liq. 78 (1–2) (1998) 83–109, http://dx.doi.org/10.1016/s0167-7322(98)00085-3.

[328] M.L. Asaki, A. Redondo, T.A. Zawodzinski, A.J. Taylor, Dielectric relaxation of electrolyte solutions using terahertz transmission spectroscopy, J. Chem. Phys. 116 (19) (2002) 8469–8482, http://dx.doi.org/10.1063/1.1468888.

[329] Z. Sun, W. Zhang, M. Ji, R. Hartsock, K.J. Gaffney, Contact ion pair formation between hard acids and soft bases in aqueous solutions observed with 2DIR spectroscopy, J. Phys. Chem. B 117 (49) (2013) 15306–15312, http://dx.doi.org/10.1021/jp4033854.

[330] S.A. Roget, K.A. Carter-Fenk, M.D. Fayer, Water dynamics and structure of highly concentrated LiCl solutions investigated using ultrafast infrared spectroscopy, J. Am. Chem. Soc. 144 (9) (2022) 4233–4243, http://dx.doi.org/10.1021/jacs.2c00616.

[331] K.K. Lee, K.H. Park, D. Kwon, J.H. Choi, H. Son, S. Park, M. Cho, Ion-pairing dynamics of Li+ and SCN- in dimethylformamide solution: Chemical exchange two-dimensional infrared spectroscopy, J. Chem. Phys. 134 (6) (2011) http://dx.doi.org/10.1063/1.3552961.

[332] V.V. Telkki, M. Urbańczyk, V. Zhivonitko, Ultrafast methods for relaxation and diffusion, Prog. Nucl. Magn. Reson. Spectrosc. 126–127 (2021) 101–120, http://dx.doi.org/10.1016/j.pnmrs.2021.07.001.

[333] M. Maiuri, M. Garavelli, G. Cerullo, Ultrafast spectroscopy: State of the art and open challenges, J. Am. Chem. Soc. 142 (1) (2020) 3–15, http://dx.doi.org/10.1021/jacs.9b10533.

[334] V. Balos, H. Kim, M. Bonn, J. Hunger, Dissecting hofmeister effects: Direct anion–amide interactions are weaker than cation–amide binding, Angew. Chem. Int. Edn 55 (28) (2016) 8125–8128, http://dx.doi.org/10.1002/anie.201602769.

[335] V. Balos, P. Müller, G. Jakob, M. Kläui, M. Sajadi, Imprinting the complex dielectric permittivity of liquids into the spintronic terahertz emission, Appl. Phys. Lett. 119 (9) (2021) http://dx.doi.org/10.1063/5.0056909.

[336] S. Funkner, G. Niehues, D.A. Schmidt, M. Heyden, G. Schwaab, K.M. Callahan, D.J. Tobias, M. Havenith, Watching the low-frequency motions in aqueous salt solutions: The terahertz vibrational signatures of hydrated ions, J. Am. Chem. Soc. 134 (2) (2012) 1030–1035, http://dx.doi.org/10.1021/ja207929u.

[337] N.Q. Vinh, M.S. Sherwin, S.J. Allen, D.K. George, A.J. Rahmani, K.W. Plaxco, High-precision gigahertz-to-terahertz spectroscopy of aqueous salt solutions as a probe of the femtosecond-to-picosecond dynamics of liquid water, J. Chem. Phys. 142 (16) (2015) http://dx.doi.org/10.1063/1.4918708.

[338] L. Chen, G. Ren, L. Liu, P. Guo, E. Wang, Z. Zhu, J. Yang, J. Shen, Z. Zhang, L. Zhou, J. Zhang, B. Yang, W. Zhang, Y. Gao, H. Zhao, J. Han, Probing NaCl hydrate formation from aqueous solutions by terahertz time-domain spectroscopy, Phys. Chem. Chem. Phys. 22 (32) (2020) 17791–17797, http://dx.doi.org/10.1039/d0cp01571g.

[339] Z.R. Kann, J.L. Skinner, Low-frequency dynamics of aqueous alkali chloride solutions as probed by terahertz spectroscopy, J. Chem. Phys. 144 (23) (2016) http://dx.doi.org/10.1063/1.4953044.

[340] A. Shalit, S. Ahmed, J. Savolainen, P. Hamm, Terahertz echoes reveal the inhomogeneity of aqueous salt solutions, Nature Chem. 9 (3) (2017) 273–278, http://dx.doi.org/10.1038/nchem.2642.

[341] D.P. Shelton, Electric field of ions in solution probed by hyper-Rayleigh scattering, J. Chem. Phys. 130 (11) (2009) http://dx.doi.org/10.1063/1.3089882.

[342] S.R. Alfarano, S. Pezzotti, C.J. Stein, Z. Lin, F. Sebastiani, S. Funke, C. Hoberg, I. Kolling, C.Y. Ma, K. Mauelshagen, T. Ockelmann, G. Schwaab, L. Fu, J.B. Brubach, P. Roy, M. Head-Gordon, K. Tschulik, M.P. Gaigeot, M. Havenith, Stripping away ion hydration shells in electrical double-layer formation: Water networks matter, Proc. Natl. Acad. Sci. USA 118 (47) (2021) http://dx.doi.org/10.1073/pnas.2108568118.

[343] H. Weiss, H.W. Cheng, J. Mars, H. Li, C. Merola, F.U. Renner, V. Honkimäki, M. Valtiner, M. Mezger, Structure and dynamics of confined liquids: Challenges and perspectives for the X-ray surface forces apparatus, Langmuir 35 (51) (2019) 16679–16692, http://dx.doi.org/10.1021/acs.langmuir.9b01215.

[344] B. Huang, Y. Yang, R. Han, K. Chen, Z. Wang, L. Yun, Y. Wang, H. Chen, Y. Du, Y. Hao, P. Lv, H. Ma, P. Ji, Y. Tan, L. Zheng, L. Liu, R. Li, J. Yang, Mapping electrostatic potential in electrolyte solution, 2023, arXiv:2311.00387.

Gareth R. Elliott is a Ph.D. student studying at the University of Newcastle (Australia) under the supervision of Prof. Alister Page, Prof. Erica Wanless and Prof. Grant Webber. He received a Bachelor of Mathematics/Bachelor of Science (Hons I) from UoN. He is currently investigating specific ion effects in various solvents at high concentrations using molecular dynamics and quantum chemical methods.

Kasimir P. Gregory obtained his Ph.D. in 2022 from the University of Newcastle under the supervision of Prof. Alister Page, Prof. Erica Wanless and Prof. Grant Webber. During his Ph.D. he investigated specific ion effects via computational and quantum chemistry. He is currently a postdoctoral researcher at the Australian National University working in the Research School of Biology under the supervision of Prof. Ben Corry. His research investigates specific ion effects, thermodiffusion and malaria via computational and quantum chemistry and biology.

Hayden Robertson Hayden graduated from a combined degree of Bachelor of Mathematics (Pure) and Bachelor of Science (Hons)(Chemistry) from the University of Newcastle in 2019. He then attained his PhD in 2024, also from the University of Newcastle, supervised by Prof. Erica Wanless and Prof. Grant Webber. His research includes investigating specific ion effects in complex environments using surface techniques such as neutron reflectometry and ellipsometry.

Vincent S.J. Craig Vince leads the Colloids group in the Department of Materials Physics at the Australian National University. He completed his Ph.D. degree jointly in the Departments of Applied Mathematics and Chemistry in 1997 at the ANU before postdoctoral positions at UC Davis, California and the University of Newcastle, NSW, Australia. His research interests include the measurement of surface forces, in particular the long range hydrophobic interaction, adsorption of surfactants and polymers, specific ion effects, wetting and bubbles, including nanobubbles. He was awarded an ARC Postdoctoral fellowship in 1998, an ARC Research Fellowship in 2001 and an ARC Future Fellowship in 2009.

Grant B. Webber is a research chemical engineer, working across discipline boundaries to uncover the links between nanoscale behaviours and macroscale properties. His research combines cutting-edge experiments and precision modelling and simulation methods to study colloidal and interfacial phenomena with relevance to personal care products, pharmaceuticals, the minerals industry, water treatment, micro- and nanomechanical devices, food production and biomedical device manufacture. Grant has deployed neutron reflection and scattering, ellipsometry, atomic force microscopy and quartz crystal microbalance measurements to resolve specific ion effects in polymer brush systems with high spatial and temporal resolution.

Erica J. Wanless is Professor and Head of Chemistry at the University of Newcastle (Australia). She graduated with a PhD in Surface Science from the Australian National University in 1995. She then completed a postdoctoral fellowship at the University of Otago, New Zealand. She joined the University of Newcastle Chemistry Department in 1996. Erica is a colloid and interface scientist who has built an international research profile for her investigations of surfactant, polymer or colloidal materials at interfaces. In recent years her research has been focussed on stimulus responsive polymer brush coatings which are tuned by changes in pH, temperature, ionic strength and/or ion identity. Erica is the current president of the Australasian Colloid and Interface Society.

Alister J. Page received his Ph.D. from the University of Newcastle in 2008. In 2009 he was awarded a Fukui postdoctoral fellowship in the group of Prof. Keiji Morokuma at the Fukui Institute for Fundamental Chemistry, Kyoto University, and in 2012 he was appointed as a Research Fellow at the University of Newcastle. He took up a faculty position in Newcastle in 2013, where he is now Professor in the Discipline of Chemistry and leads the University of Newcastle Computational Chemistry Group. His research focuses on developing and applying quantum chemical methods to topics including self-assembly, carbon & inorganic nanomaterials, ionic liquids, deep eutectic solvents, heterogeneous & photocatalysis, and specific ion effects.